

**A STUDY OF SINGLE PLANAR RESONATOR FOR DIELECTRIC
CHARACTERIZATION**

ABDIQUDUS ABUBAKAR MOALIM RASHID



UNIVERSITI TUN HUSSEIN ONN MALAYSIA

STATUS CONFIRMATION FOR MASTER'S PROJECT REPORT

A STUDY OF SINGLE PLANAR RESONATOR FOR DIELECTRIC CHARACTERIZATION

ACADEMIC SESSION: 2020/2021

I, **ABDIQUDUS ABUBAKAR MOALIM RASHID**, agree to allow this Master's Project Report to be kept at the Library under the following terms:

1. This Master's Project Report is the property of the Universiti Tun Hussein Onn Malaysia.
2. The library has the right to make copies for educational purposes only.
3. The library is allowed to make copies of this report for educational exchange between higher educational institutions.
4. The library is allowed to make available full text access of the digital copy via the internet by Universiti Tun Hussein Onn Malaysia in downloadable format provided that the Master's Project Report is not subject to an embargo. Should an embargo be in place, the digital copy will only be made available as set out above once the embargo has expired.
5. ** Please Mark (✓)

CONFIDENTIAL

(Contains information of high security or of great Importance to Malaysia as STIPULATED under the OFFICIAL SECRET ACT 1972) *Title and Abstract only*

RESTRICTED

(Contains restricted information as determined by the Organization/institution where research was conducted) *Title, Abstract and Introduction only*

EMBARGO

_____ until _____
(date) (date)

FREE ACCESS

Approved by,

(WRITER'S SIGNATURE)

(SUPERVISOR'S SIGNATURE)

MR. EZRI BIN MOHD

Permanent Address:

NO 11, TAMAN WIRA,
86400 PARIT RAJA
BATU PAHAT, JOHOR.

Date: _____

Date: _____

NOTE:

** If this Master's Project Report is classified as CONFIDENTIAL or RESTRICTED, please attach the letter from the relevant authority/organization stating reasons and duration for such classifications.

ASTUDY OF SINGLE PLANAR RESONATOR DOR DIELECTRIC
CHARACTERIZATION

ABDIQUDUS ABUBAKAR MOALIM RASHID

A project report submitted in partial
fulfillment of the requirement for the award of the
Degree of Master of Electrical Engineering

Faculty of Electrical and Electronic Engineering
Universiti Tun Hussein Onn Malaysia

FEBRUARY 2021

I hereby declare that the work in this project report is my own except for quotations and summaries which have been duly acknowledged

Student : ABDIQUDUS ABUBAKAR MOALIM
RASHID

Date : 10 FEBRUARY 2021

Supervisor : MR. EZRI BIN MOHD



PTTA UTHM
PERPUSTAKAAN TUNKU TUN AMINAH

ACKNOWLEDGEMENT

I want to express my utmost gratitude to Allah the Almighty Allah the Most Gracious and most Graceful. Alhamdulillah. For me to work on this Project was a valuable experience. I would like to express my sincere thanks and gratitude for giving me the opportunity to work and advise my supervisor Mr. Ezri Bin Mohd, and my co-supervisor Associate Professor Dr. Noorsaliza Binti Abdullah. I would like to thank the people who gave me their assistance and guidance in my project period under their supervision. Thank you for support me. My Allah's blessing and guidance be with you.



PTTA UTHM
PERPUSTAKAAN TUNKU TUN AMINAH

ABSTRACT

A square split-ring resonator (SSRR) for dielectric characterization for solid materials such as Wood and Iron is proposed. The SSRR is design on the substrate, material of FR4 and copper for the square ring, copper on ground. The dielectric characterization sensor is depends on the change of the resonance frequency and change material sample mounted on the resonator. The simulated s-parameter response of a single square SRR. Simulated design started by designing a square split ring resonator with no gap and two feedlines on both sides which connects to port one and port two, S11 at 3 dB and S21 at 14 dB .Then, start modifying the design of square SRR by cutting gap on both sides of square ring. The simulated result of modified square SRR at S11 -35 dB and S21 -2.5dB both started design and modified at frequency of 2.45 GHz. Material under test MUT started with placing sample on the most sensitive area of permittivity and permeability. Solid material such as iron and wood have been used in this simulation the iron which makes the frequency moves from 2.45 GHz with -35dB to 2.26 GHz with -13dB, wood which makes the frequency moves from 2.45 GHz with -35dB to 2.497 GHz with -23.6dB. Both of this results verified that the SRR design is working as sensor.

TABLE OF CONTENTS

| | |
|---|-------------|
| TITLE | I |
| DECLARATION | II |
| ACKNOWLEDGEMENT | III |
| ABSTRACT | IV |
| TABLE OF CONTENTS | V |
| LIST OF TABLES | VII |
| LIST OF FIGURES | VIII |
| CHAPTER 1 | 1 |
| 1.1 Background | 1 |
| 1.2 Problem Statement | 2 |
| 1.3 Objectives | 3 |
| 1.4 Scope of Study | 3 |
| 1.5 Organization of thesis | 3 |
| CHAPTER 2 | 4 |
| 2.1 Introduction | 4 |
| 2.2 Dielectric measurement techniques | 5 |
| 2.3 Non resonant techniques | 5 |
| 2.3.1 Waveguide and coaxial transmission line techniques | 6 |
| 2.3.2 Free space transmission techniques | 7 |
| 2.3.3 Open ended transmission line method | 8 |
| 2.3.4 Planar transmission line techniques | 10 |
| 2.4 Resonant methods | 11 |
| 2.4.1 Waveguide cavity resonators | 12 |
| 2.4.2 Coaxial cavity resonators | 13 |
| 2.4.3 Open ended resonant lines | 14 |
| 2.4.4 Planar transmission line resonators | 14 |
| 2.5 Types of Resonators Used Across the RF/Microwave Universe | 16 |

| | | |
|-------------------|---|-----------|
| 2.5.1 | Coaxial Resonators | 17 |
| 2.5.2 | Dielectric Resonators | 17 |
| 2.5.3 | Crystal Resonators | 18 |
| 2.5.4 | Ceramic Resonators | 19 |
| 2.5.5 | Saw Resonators | 19 |
| 2.6 | Materials of dielectric resonator | 20 |
| 2.7 | Application for dielectric resonator | 20 |
| 2.8 | Previous Work Study | 20 |
| 2.9 | Summary | 24 |
| CHAPTER 3 | | 25 |
| 3.1 | Introduction | 25 |
| 3.2 | Flowchart | 25 |
| 3.3 | Substrate Specification | 27 |
| 3.4 | Project Methodology | 27 |
| 3.4.1 | Calculation | 28 |
| 3.4.2 | Simulation | 30 |
| 3.4.3 | Square split Ring Resonator | 30 |
| 3.4.4 | Square Split Ring Resonator with Gap | 32 |
| 3.4.5 | Split Ring Resonator Technique | 33 |
| 3.5 | Dielectric Characterization Design for Material | 34 |
| CHAPTER 4 | | 36 |
| 4.1 | Introduction | 36 |
| 4.2 | Simulation Result and Discussion | 36 |
| 4.2.1 | Square split Ring Resonator | 36 |
| 4.2.1.2 | Square Split Ring Resonator with gap | 37 |
| 4.3 | Current Distribution | 39 |
| 4.4 | H-field and E-field distribution of the Square split Ring Resonator | 39 |
| 4.5 | Square split Ring Resonator Parametric study analysis | 40 |
| 4.6 | Result of Dielectric characterization for materials | 43 |
| CHAPTER 5 | | 47 |
| 5.1 | Summary | 47 |
| 5.2 | Recommendation | 48 |
| REFERENCES | | 49 |

LIST OF TABLES

| | |
|---|----|
| 3.1: Substrate Materials Specification | 27 |
| 3.2: The specification of the SRR | 30 |
| 3.4 Specification of ring and feedline | 30 |
| 3.5 Specification of square ring with gap | 32 |
| 4.1: Parametric study of Ring gap | 40 |
| 4.2: Parametric study of feedline gap | 41 |
| 4.3: Parametric study of Ring width | 42 |



LIST OF FIGURES

| | |
|--|----|
| 2.1: (a) Waveguide fixture and (b) Coaxial fixture for transmission measurements. | 6 |
| 2.2: Typical arrangement of a free space dielectric measurement setup. | 7 |
| 2.3: Open ended coaxial and waveguide transmission lines. | 8 |
| 2.4: Dielectric waveguide fixture for the complex permittivity measurement of low dielectric constant materials. | 9 |
| 2.5: Microstrip cell for complex permittivity measurement of liquids. | 11 |
| 2.6: Coplanar waveguide cell for complex permittivity measurement of liquids. | 11 |
| 2.7: Coplanar waveguide cell for complex permittivity measurement of liquids | 13 |
| 2.8: Waveguide cavity resonators for complex permittivity measurements. | 13 |
| 2.9: Open-ended resonant line for complex permittivity measurements. | 14 |
| 2.10: Microstrip fixture for resonant perturbation measurements on liquid samples. | 16 |
| 2.11: resonator sensor for complex permittivity measurements. | 16 |
| 2.12: This illustration represents a typical disc-shaped dielectric resonator. | 18 |
| 3:1 Flowchart of the project | 26 |
| 3.2: (a) Substrate (b) ground of basic SSRR | 31 |
| 3.3: (a) Substrate (b) Ground split ring resonator. | 32 |
| 3.4: (a) Basic SRR (b) modified SRR. | 33 |
| 3.5: S parameter (a) Basic (b) modified SRR. | 34 |

| | |
|---|----|
| 3.6: Original design. | 35 |
| 3.7: Iron sample for MUT | 35 |
| 3.8: Wood sample for MUT | 35 |
| 4.1: Square SRR | 37 |
| 4.3: Modified Square SRR | 38 |
| 4.4: Simulated S-parameter of Modified Square SRR. | 38 |
| 4.5: Distribution of electric field at the Square SRR frequency of 2.45 GHz. | 39 |
| 4.6 Permeability and Permittivity sensing area | 40 |
| 4.7: Simulated S-parameter parametric study of ring gap. | 41 |
| 4.8: Simulated S-parameter parametric Study of feedline gap. | 42 |
| 4.9: Simulated S-parameter parametric Study of Ring width | 43 |
| 4.10: The result before MUT | 44 |
| 4.12: The simulation after wood sample tested | 45 |
| 4.13: S11 Comparing the result of material befor and after MUT. | 45 |
| 4.14: Compare of before and after MUT. | 46 |



CHAPTER 1

INTRODUCTION

1.1 Background

Square split ring resonator for dielectric characterization, first start design SSRR for sensor. Establish simulate the SRR and do parametric study to get good frequency. The electromagnetic properties of materials are characterized from the two after constitutive boundaries: permittivity and permeability.

In this project MUT sample is placed is most sensitive area of SRR for detecting the material and will mainly focus on solid material such as Iron Wood and compare them with the original dielectric resonator sensor before material under test.

As a rule, to quantify the permittivity and permeability of a given material, a model is put in transit of a traveling electromagnetic wave, either in free space or inside one of the propagation structures referenced. Material characterization strategies counts on RF and microwave measurement have been extensively utilized these reasons. These strategies can be named free-space estimations, transmission line, and resonance-based methods. Cavity resonators are commonly applied in this philosophy; regardless, recently, split-ring resonators (SRRs), and complementary split-ring resonators (CSRRs), have been considered as promising options. In SRR or CSRR based sensors, a microstrip transmission line is stacked with a SRR or CSRR [1]-[2].

Characterization of the real and imaginary parts of the electric permittivity of materials utilizing SRR and CSRR based sensors has been wildly thought to be in past studies, so to our best data, extricating both the

permittivity and permeability of dielectric material utilizing a resonator-based sensor. In these works, two distinctive SRRs were applied, one for acknowledgment of electric permittivity and one for attractive porousness. Fundamentally, in the two works, Simulate Square split ring resonator and test sample solid material such as iron and wood to verify the sensor is working on both materials [4]-[9].

1.2 Problem Statement

Precise affirmation of the permittivity and permeability of materials is huge in various areas, for instance, food production, agriculture, medication and human health administrations, and military and defense. The resonance-based procedures are consistently preferred because of the high accuracy, high sensitivity and low expense. After simulation the material test the frequency will shift reacting to which material is tested [10]-[13].

The test in the synchronous recovery of the permittivity and permeability of a dielectric material using the resonance-based detecting approach is that both the permittivity and permeability of the MUT bring about shifting of the SRR frequency.

Consequently, one cannot perceive impacts of the permittivity and permeability in the change in the resonance frequency. The basic idea behind this work is to limit the electric and magnetic fields in two separate zones of a SRR in a way that in a domain of the SRR, the attractive field is localize with a high power while the electric field has an incredibly low strength; thusly, this zone can be used for detecting of magnetic permeability.

Sample of material will be placed on most sensitive area of SRR to test the change of frequency comparing them with before testing.

Finally design of SRR hast to work as sensor an verify both materials are working

1.3 Objectives

The objectives of this project are:

1. To design Square SRR for dielectric characterization.
2. To analyze the resonator performance in terms of S_{11} and S_{21}
3. To study the localized E-field & H-field with good isolation.

1.4 Scope of Study

This project major phase:

- i. Study single planar resonator for dielectric characterization in general.
- ii. a review of previous design will be analyzed and studied in order to have a knowledge related to this title, which is the dielectric resonator design techniques, different structures and shapes,
- iii. To produce strongly localized E-field & H-field with good isolation between these field
- iv. Design of SRR and MUT simulation.
- v. CST software will be used to design and simulated resonator.

1.5 Organization of thesis

Chapter 1 describes the motivation for doing this project. The objectives are stated and the organization of the thesis is shown in this chapter, chapter 2 will give an overview of this project and briefly, introduction for resonator and dielectric will be given. Particularly, explaining the general idea about the topic, types of resonator and dielectric, chapter 3 will propose SSRR basic resonator and modifications and material testing, will focus on CST design, chapter 4 will focus on result and discussion.

CHAPTER 2

LITERATURE REVEIW

2.1 Introduction

A dielectric material (dielectric for short) is an electrical insulator that must be energized by applying an applied electric field. At whatever point a dielectric is set in an electric field, the electric charge quits going through the material, yet a slight shift from their normal equilibrium positions causes dielectric polarization.

The term dielectric is utilized to indicate the energy storage capacity of a material. An illustration of a dielectric is setting a ceramic material between the metal plates of a capacitor. In the event that the voltage of a dielectric material turns out to be too high or the electrostatic field turns out to be too strong, the material will out of nowhere begin turning current. This cycle is called dielectric breakdown. A significant property of a dielectric is its capacity to withstand an electrostatic field while dissipating minimal energy in the form of heat. The less dielectric loss of the material, the more powerful the dielectric material. The second interesting point is the dielectric constant, which describes the degree to which the electrostatic lines of matter flow. A few substances with low dielectric consistent have full vacuum, dry air and the perfect, dry gases like helium and nitrogen. Materials with moderate dielectric constants consist of ceramic, distilled water, glass; and so on, most metal oxides have high dielectric stability. The investigation of dielectric properties manages the capacity and scattering of electrical and magnetic energy rays of materials. Dielectric stunts are significant for clarifying the different types of electronics, optics and solid-state physics.

2.2 Dielectric measurement techniques

Estimation strategies of ideal system comes from the idea of the dielectric material to be estimated electrically and naturally, the frequency of interest, and the degree of accuracy required. Having the option to produce the correct case for the model, getting a sufficient sample of the circuit for solid calculation of the remittance from power estimations ends up being a significant test. In low and medium frequency ranges, bridge and resonance circuits are frequently used to characterize dielectric materials. In any case, at high frequency, diffusion line, resonant cavitation and free-space strategies are ordinarily utilized and depicted in the underlying audit (Altschuler, 1973). For the most part, dielectric estimation methods can be classified as reflection or transmission type, utilizing system that do not resonate or resonate. [14].

2.3 Non resonant techniques

On account of non resonant modes, the materials effects are essentially founded with respect to the resistance and their wave velocity. At the point when an electromagnetic wave is transmitted from point to point, the change come from waves both impedance and velocity, bringing about partial wave reflection by interconnection both materials. Reflections estimations and propagation from such port give data to get permittivity and permeability connections both objects. Non resonant modes for the most part incorporate reflection and reflection / diffusion modes.

In this strategies for reflection, the specification of the item is gotten from both phase,size estimation of the signal that is reflected. In reflection / diffusion estimations, the specification of this material are gotten from both phase, size estimation of the reflected and sent signals. To modify trust of the outcomes, so for the most part wanted to utilize results from reflection and diffusion estimations. Non resonant modes need a strategy to coordinate electromagnetic energy onto the item and to gather and reflect and transmit it. Any kind of transmission line can be utilized for

this reason; For instance, coaxial line, hollow metallic waveguide, planar transmission line and so on [15].

2.3.1 Waveguide and coaxial transmission line techniques

In non-resonant mode, the sample to be tested is put in a segment of the transmission line, which is generally a waveguide or coaxial line. The electromagnetic properties of the tested materials, their straightforwardness, can be acquired from the scattering parameter. In this manner four dispersing parameter can be estimated. For complex permittivity and permeability, the places of the two reference planes and the model length are the primary factors remembered for the dispersion equation for estimating dissemination or reflection.

In spite of the fact that the cut wave f wavelength length of a coaxial line is endless, setting an example on a coaxial line, particularly a rectangle shape, is harder and directs to the utilization of waveguides. Figure 2.1 shows the cross part of a rectangular waveguide with the sample set up. Filling the line and leaving space is normally the estimation setting. It shows the direction of axis in the X direction. This is equivalent to direction of propagation. [16].

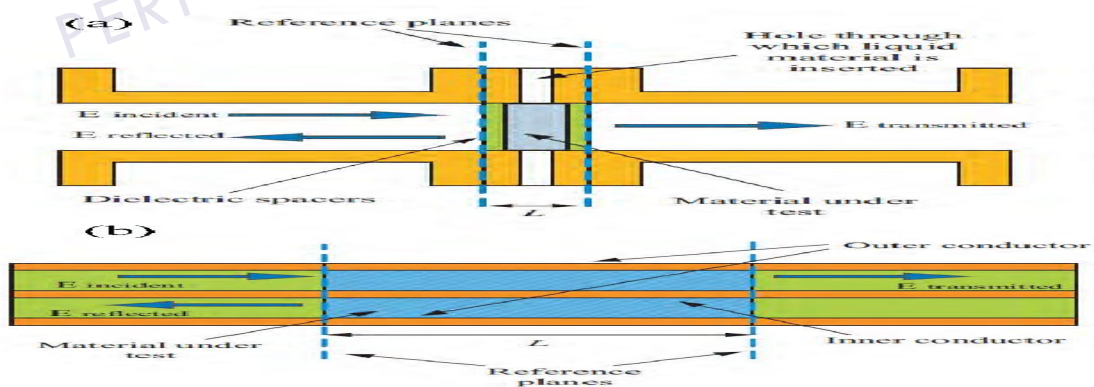


Figure 2.1: (a) Waveguide fixture and (b) Coaxial fixture for transmission measurements.

2.3.2 Free space transmission techniques

Precise assessments can be performed in free space at microwave frequencies to supply accurate get to a horn point of convergence receiving wire with the capacity to focus middle within the distant field. The use of good systems to degree physical properties offers a few central points, explicitly that undesired higher arrange modes at the air-dielectric interface can be stimulated in empty metal waveguides, which enables materials, such as clay and ceramic to be destroyed, while this issue doesn't arise when estimating free space is available.

At that point, it can be utilized to measure samples at tall temperatures and does not have to set up the tests to arrange the waveguide cross-section with little holes, which can be used to limit the exactness of assessment for these materials.

There are necessities that cannot be really watched out for, for example, the empty metal waveguide system. Figure 2.2 shows up an ordinary free space assessment set up, which fundamentally involves two-horn lens antenna and a test to be attempted (MUT).

Lens antenna is for spot centering to limit the impacts of sample limits and estimation invironmen (Chen et al., 2004), (Rustam, 2013), and (Varadan et al., 2003) [17].

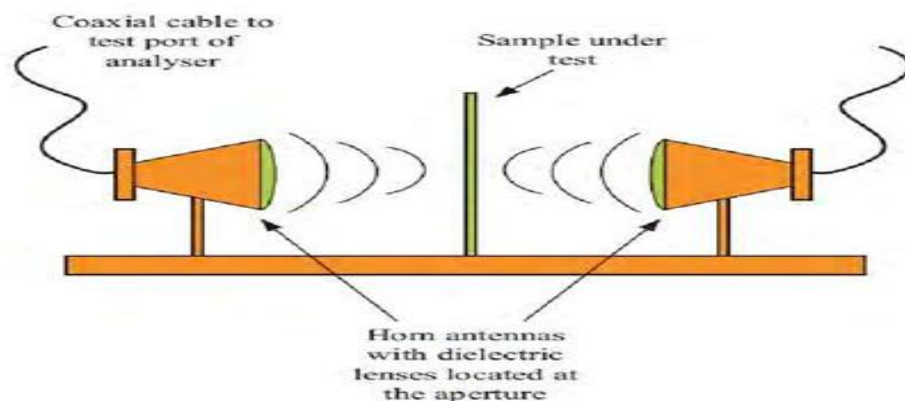


Figure 2.2: Typical arrangement of a free space dielectric measurement setup.

2.3.3 Open ended transmission line method

This transmission line methods give an accommodating and a non-intrusive establishment for the assessment For the assessment of dielectric permittivity of liquids including semi-solids without test planning. Stuchly and Stuchly (Athey, 1982) introduced this approach, using it to determine the dielectric properties of natural materials. For long term, this method was advanced. For this system, the tested material was set at the opposite region of cut-off for the transmission line, including maximum and phase for reflected sign are estimated Figure 2.3.

A few models were used over the previous decade or so to link the permittivity of the fabric to the approximate reflection coefficient at the opening of the probe.

We use waveguide and coaxial transmission lines, Since they are extremely broadband and have no figures, regardless of how coaxial lines are best.

The system appropriated for estimating both high dielectric constant and loss tests, so the method for characterizing Lossy surfaces and solvents. It calls for reference planes for calibration to be gotten from test opening, which are trying on account of a coaxial test. Notable reference materials are regularly needed for calibration [18].

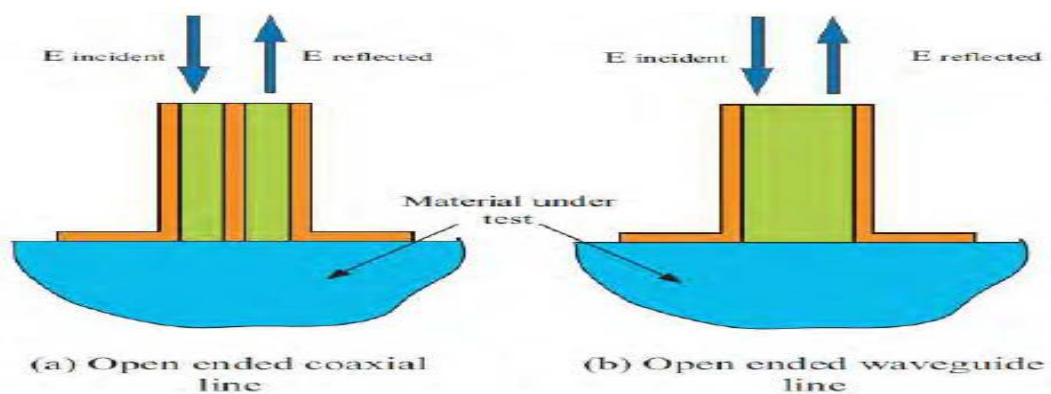


Figure 2.3: Open ended coaxial and waveguide transmission lines.

Dielectric waveguide techniques as of late, dielectric waveguide processes (Abbas, 2001) have been proposed that allow the assurance of dielectric permittivity of low loss planar sheet materials, such as Teflon or Perspex, to be guaranteed. The sample to be estimated is positioned in direct contact between two circular or rectangular geometric dielectric waveguides Figure 2.4. The sample may have an arbitrary form, but its transverse dimension should be more noteworthy than the transverse dimension of the dielectric waveguide, or, in the limiting case, equivalent.

Two fundamental properties of dielectric waveguides are depending on the device. The primary property is that inside the waveguide, the energy of the wave propagating inside the waveguide is totally centered. The other asset is that the phase velocity is an equivalent design demonstration that can be used in verification of the complex permittivity from reflection and transmission estimates (Abbas, 2001).

Suitable changes are necessary in order to dispatch energy into a dielectric waveguide. These are developed mainly using metallic horn antennas that can be difficult to design [19].

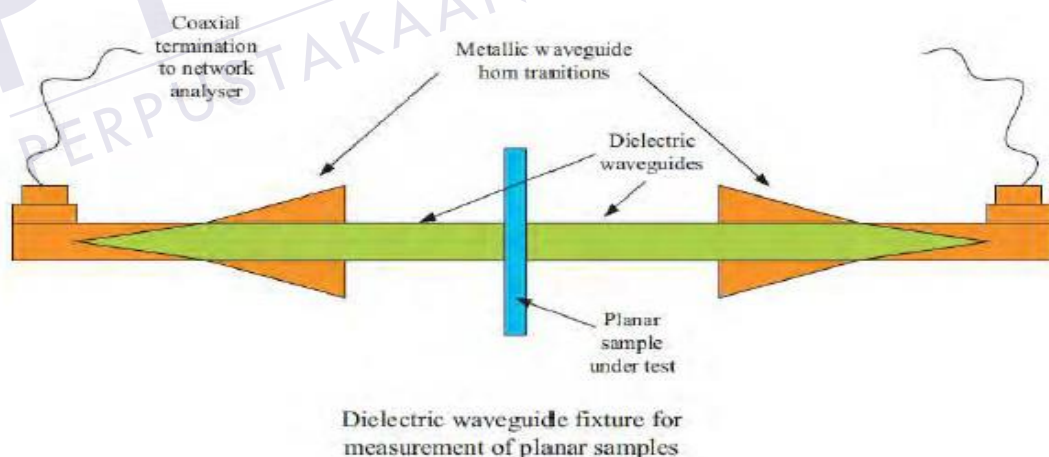


Figure 2.4: Dielectric waveguide fixture for the complex permittivity measurement of low dielectric constant materials.

2.3.4 Planar transmission line techniques

Planar transmission lines, for example, microstrip and coplanar waveguides have for quite some time been utilized as microwave parts. They permit simplicity of fabrication, cheap, and Compactness, which makes them ideal for industrial applications that use estimations of dielectric permittivity. The material to be examined usually fills in as a superstrate or as a substrate, or as part of both, in planar transmission line techniques. The dielectric sample may serve as both the substrate or the superstrate on account of solids. In any event, it is easier to have the sample as a superstrate on account of liquids and semi-solids.

Numerous examinations have been carried out concerning the use of planar circuits for complex liquid permittivity estimations (Stuchly, 1998, Raj, 2001, Facer, 2001, Queffelec, 1994, Hinojosa, 2001, Wadell, 1991, Chen, 2004). Figures 2.5 and 2.6 indicate standard planar cells for liquid material dielectric permittivity estimations. The liquid to be estimated occupies the whole of the planar circuit and is placed within a low-loss compartment, which is fixed, or epoxy dated to the top of the board. The area fenced provides mismatches that can certainly be calibrated. The liquid dielectric presentation modifies the efficient of permittivity and the characteristic Z_0 of the line. The dielectric properties are then obtained from the change in effective permittivity utilizing reasonable expressions that can be found in the literature (Wadell, 1991) [20].

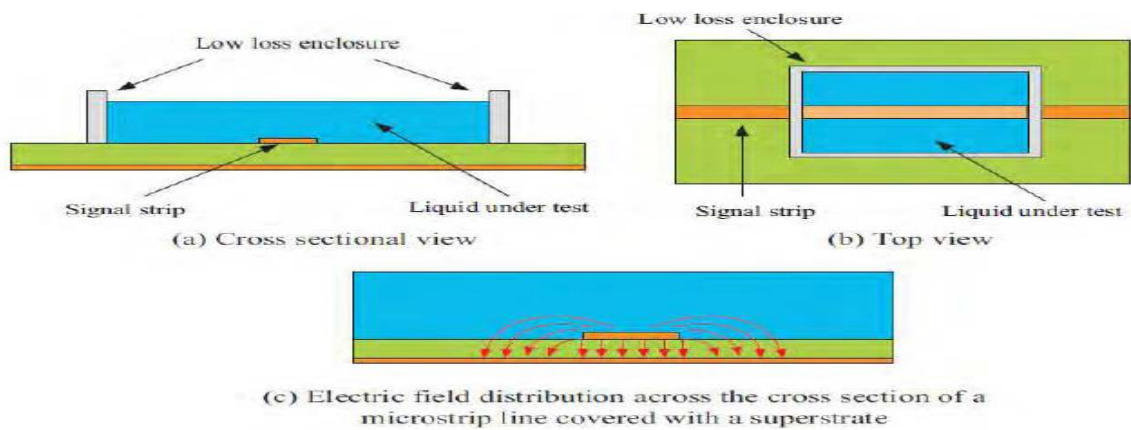


Figure 2.5: Microstrip cell for complex permittivity measurement of liquids.

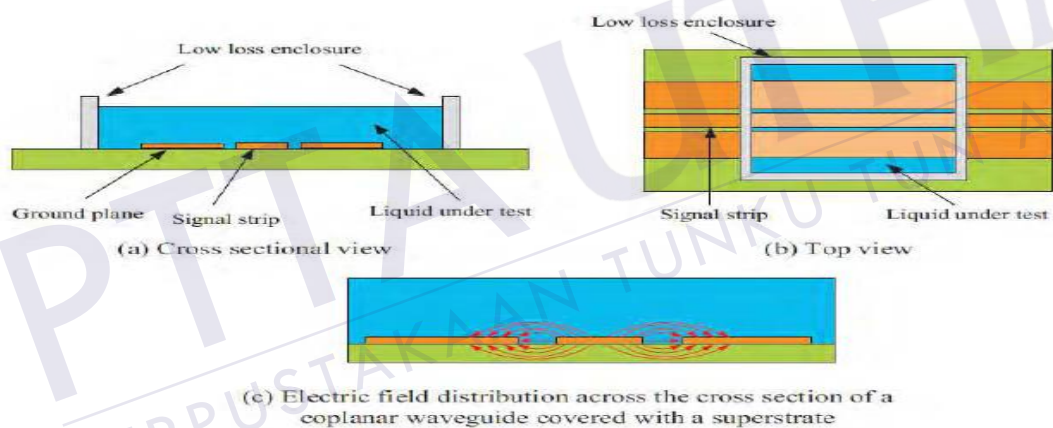


Figure 2.6: Coplanar waveguide cell for complex permittivity measurement of liquids.

2.4 Resonant methods

In contrast with the broadband methods, resonant methods give the ability to describe the characteristics in a single frequency or discrete range of frequencies with high precision. They can be categorized into methods of resonator and resonant disruption. The resonator methods shall only refer to extremely low loss samples when the substance to be measured acts as a resonator. The various resonant forms used in this field can also

be categorized into dielectric, coaxial surface waves and divided resonators. You can find information about these approaches in (Chen, 2004). Resonant disturbance approaches include those in the resonant structure in which the sample reaches the response and causes disturbance. The interference results in a change in the frequency of the resonant and in a reduction in the unloaded efficiency factor of the resonator, which measures the dielectric properties. The resonant disruptive technique is suitable for samples with low and medium loss. For this reason, resonators of reflection and transmission form may be used [21].

2.4.1 Waveguide cavity resonators

Waveguides cavity resonators are widely used for high-quality resonance disturbance estimates. Resonant cavities are designed by normal electromagnetic field spreading methods TM (transverse magnetic) or TE (transverse electrical). The cavity decision used relies on the distribution of interest in the particular area. The substance to be examined is incorporated into a special region of the cavity with the highest electrical field. A rod-shaped sample is routinely used and the sample is supposed to be preserved due to fluid and semi-solid materials.

By including the sample inside the cavity, the device disrupts and reduces the unloaded quality factor, contributes to a change in resonant frequency. This disturbance in the cavity's reaction is recognized by materials due to the theory of cavity disruption, which is the best known approach attributed to their simplicity and precision. The cavity should be built for a certain frequency and cavity resonators should be regularly wide at lower frequencies. Figure 2.7 demonstrates the TE₁₀₁ rectangular and cylindrical TM₀₁₀ waveguides in the two most commonly used allow ability spreads for permittivity estimations [22].

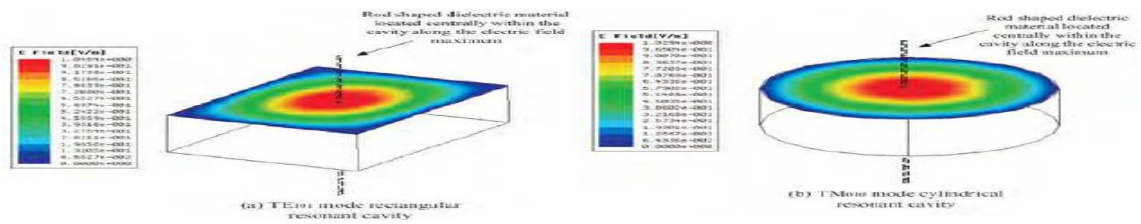


Figure 2.7: Coplanar waveguide cell for complex permittivity measurement of liquids

2.4.2 Coaxial cavity resonators

For complex permittivity figures of both moderate and high percentages a coaxial cavity shown in Figure 2.8 can also be used. Raveendranath and its associates have shown this approach (Raveendranath, 2000) and can also be investigated using the principle of disturbances. It has fantastic variables, so that failure samples can be calculated. The coaxial cavity resonator effectively is a direct coaxial line, connected with a coaxial line from one end and shortened or left open from the other end.

With only one electric field and multiple higher ordering resonances, the box shows resonance at the crucial one, that could also be used for estimates at discrete frequencies. The cavity is inserted by a rod-shaped material, which can be glided along the length of the cavity, into the external conductor. Because of the existence of coaxial lines as broadband, a very large bandwidth is available for resonant estimates [23].

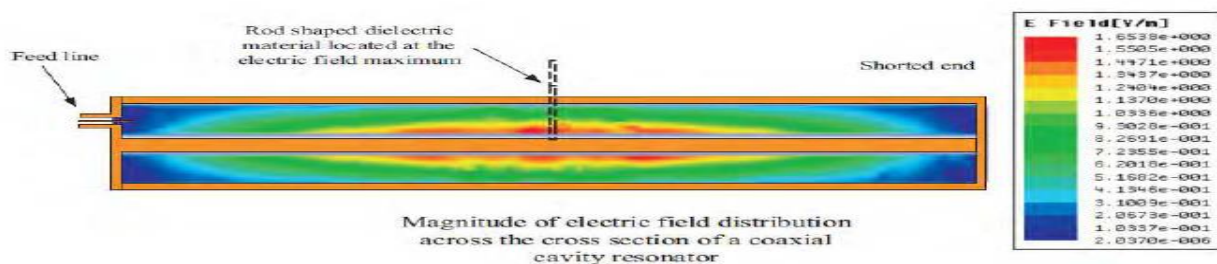


Figure 2.8: Waveguide cavity resonators for complex permittivity measurements.

2.4.3 Open ended resonant lines

However, the resonant open end line strategy initially demonstrated by Johnson and his associates is not all the important resonant technology used for complex permittivity estimates (Johnson, 1992). This sensor consists of the long line with the feed input line, which is distant from the shorter end $L_1 = \lambda/2$, with $L_2 = \lambda/2$ from the open end (figure 2.9). The fields are collected at the resonator's open end gap when the the sample to be measured touches the material. This technique is obviously useful for estimating samples with high losses and does not include preparations for samples.

Before the sensor contacts the test material, the sensor is adjusted in the air. The effect of the material on the sensor gap deflects the reaction. The reaction is then reconnected with the change in length L_1 to the first frequency. This duration modification is directly consistent with the material's permittivity.

The breakdown of the resonator's quality factor after tuning results in sample loss data[24].

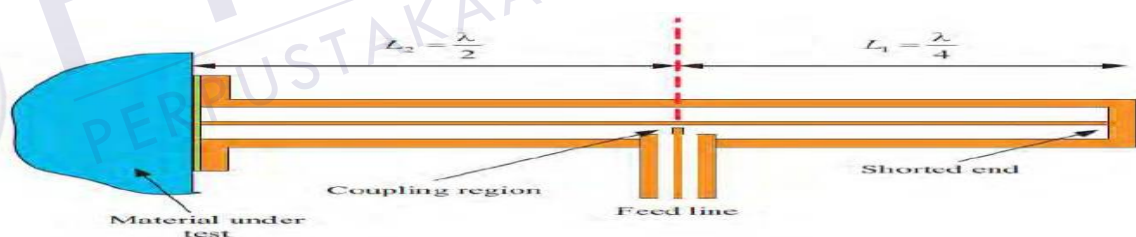


Figure 2.9: Open-ended resonant line for complex permittivity measurements.

2.4.4 Planar transmission line resonators

For permittivity calculations, virtually any kind of planar topology can be used. Tragically, any planar method has low quality factors (less than 500) and the result was common in low to direct losses. Similarly, the

example under analysis is either a substrate, or superstrate, or both in terms of broadband planar transmission line techniques, in planar resonator disruption measurements.

The device disturbance is controlled by the example properties and the degree of contact with the electrical fields. Figure 2.10 shows Abdunour and partners' planar straight strip resonator microstrip (Abdunour, 1995). (Abdunour, 1995). This arrangement is ideal for measurements of fluid samples for resonant disturbances. The sample is inserted in the substratum in a tiny opening.

Since the electric fields converge more at the resonator tips, the sample could be at the ends of the sample. The electrical fields comply with the dielectric system and induce a capacitive reaction disorder. For characterization, the advantage of using such a technique is your limited amount of samples (less than a hundred microliters). This is especially useful, for example in the pharmaceutical industry where accurate material characterization in small quantities is crucial. The Boosanovich [Bogosanovich, 2000] suggested another major resonant microstrip for relatively loosy samples.

The sensor is essentially a circular disk resonator that is attached to the coaxial line that runs from the base through the substratum. Figure 2.11 lists the approximate environment. The calculated sample is used as a superstrate and the dielectric properties of the resonation change and the quality factor of the reaction are estimated. The sampling size needed for estimates is largely huge at low frequencies, since the material must cover the patch entirely. The articulation of closed structures enables the permittivity to be defined without any calibration samples of references.

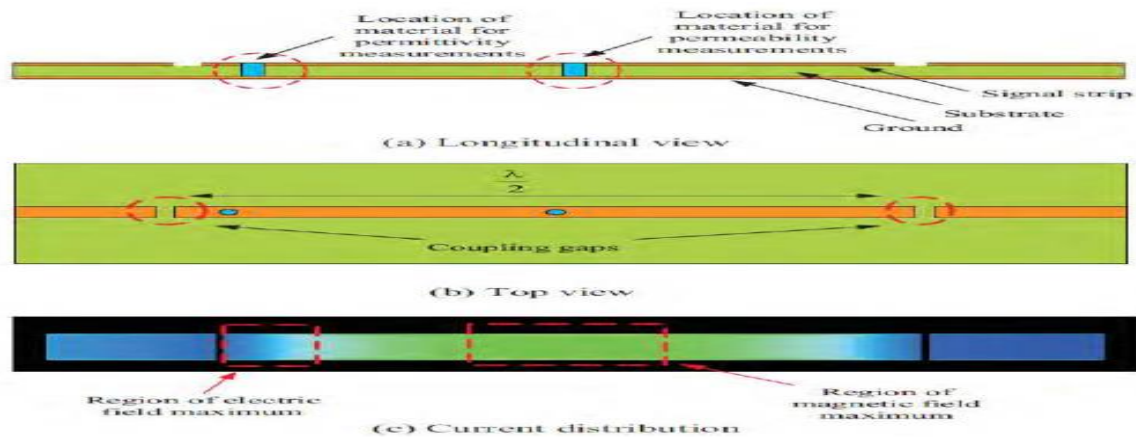


Figure 2.10: Microstrip fixture for resonant perturbation measurements on liquid samples.

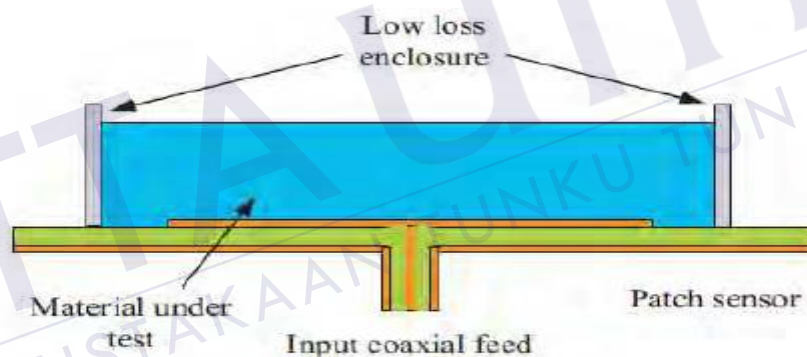


Figure 2.11: resonator sensor for complex permittivity measurements.

2.5 Types of Resonators Used Across the RF/Microwave Universe

Resonators, for example oscillators and filters, are important for the presentation of the spectrum of RF/microwave components. Coaxial, dielectric, crystal, ceramic, acoustic surface waves and Yttrium iron garnets are the types of open resonators (YIG). Given these variations, designers must consider the features of the various resonators.

2.5.1 Coaxial Resonators

Coaxial resonating systems are generally used for designing components such as tensile oscillators (VCOs, CROs), and channels. The resonator of this kind is essentially a coaxial ceramic line. Coaxial resonators are sometimes performed as high quality (high-Q) inductors with oscillators, which then generate a resonant circuit in combination with a condenser or varactor diode. An external conductor with an approximately square cross part and a cylindrical core conductor is required for a coaxial resonator.

There are two distinct configurations of coaxial resonators: quarter-wavelength resonator ($\lambda/4$) with a short, far edge end and a resonator with a half-wavelength ($\lambda/4$) with the two open ends. Since the material of a coaxial resonator has a high dielectric constant (ϵ_r) value, the parts built can be kept as small as possible. The standard ϵ_r values vary between 10 and 100.

The sizes are seven and the values four μr . These resonators are provided by the company for applications from ultra-high frequency (UHF) to 6 GHz. Tusonix also sells ceramic coaxial resonators. These products are available in four sizes and 4 range values by the organization. It is 800 MHz up to 5.9 GHz. They will have oscillators, filters and duplexer in their intended applications. Meanwhile, Temex Ceramics provides a product range of coaxial resonators for military and space, automotive, wireless and telecommunication applications. Applications from 300 MHz to 6 GHz are possible with resonators. In addition, choices can be made with several values in different dimensions.

2.5.2 Dielectric Resonators

For adjusting the cavities of components like filters and oscillators, a dielectric resonator can be used. It is typically disc-shaped with a high respect. it is usually a substance. This great esteem gives the size of a circuit board with a dialectical resonator a greatly favorable location that makes it fully smaller than when using a cavity-filled air resonator.

Electromagnetic fields are largely limited to a dielectric resonator, allowing small and high-quality radiation misfortunes (Q) to be performed Figure 2.12.

Despite the fact a dielectrical resonator can reverberate in certain modes, a large number of applications are most commonly used in $TE_{01\beta}$ (transverse electrical) mode. A dielectric resonator could be attached magnetically to a circuit with a variety of specific techniques when operating in this mode. One approach is to connect the resonator with a pathway. This approach can be used to manufacture components such as dielectric oscillators (DROs) [25].

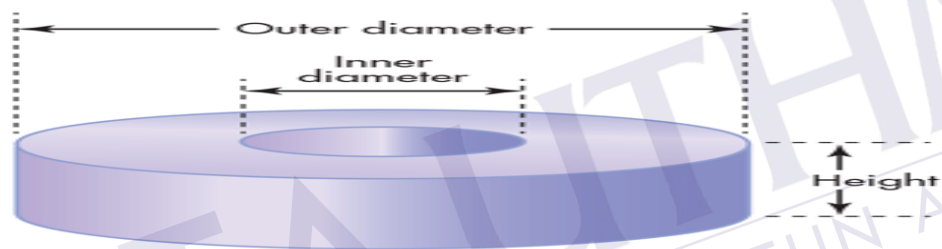


Figure 2.12: This illustration represents a typical disc-shaped dielectric resonator.

2.5.3 Crystal Resonators

The crystal of the quartz may be used as large resonators. The piezoelectric characteristics allow them to be used in crystal oscillators as frequency control components. Quartz crystals have high Q and overwhelming reliability. In fact, their high Q is the key motive behind the frequent use of quartz crystal oscillators rather than LC oscillators.

Piezoelectric materials can change electricity and otherwise over mechanical energies. An electrical charge is produced when a mechanical pressure is applied. This electrical charge matches the mechanical pressure applied. When an electric field is applied, a related substance becomes strained [26][27].

2.5.4 Ceramic Resonators

In quartz crystals, ceramic resonators are an option. While being less reliable than quartz crystals, ceramic resonators provide a variety of benefits. For example, small packages and lower cost can be generated. They offer more than quartz crystals a less start-up period.

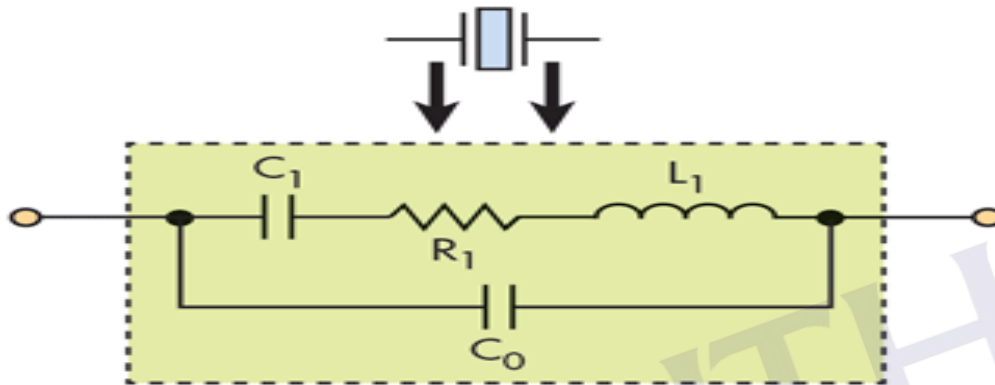


Figure 2.13: This electrical circuit represents a quartz crystals electrical equivalent near a resonant frequency.

Ceramic resonators use piezoelectric ceramics' mechanical resonance, such as plum zirconium titanate (PZT). On both the top and bottom portion of the ceramic substratum, two metal conductors are equally placed.

2.5.5 Saw Resonators

A piezoelectric crystal proliferating surface wave (SAW) can be used for transmitting data. An inter-digital transducer and two collecting reflectors are used in a fundamental SAW resonator, which is generated by photolithography on a piezo electrical content.

2.6 Materials of dielectric resonator

The manufactured sensor shows resonant frequency at 2.45 GHz and the simulated results. Tests of Dielectric (FR4 and copper) and dielectric materials such as iron and wood were readied. From each MUT, two cuts on both sides to the detecting regions for the permittivity and permeability. The use of a vector network analyser in the test setup was calculated by stacking the sensors with different samples on most sensitive are of SRR. The sensor's deliberate S11 and S21 is arranged individually when different spectrums are stacked in areas for permeability detection. The unpredictable permittivity (ϵ_r and $\tan \delta_e$) and permeability (μ_r and $\tan \delta_m$) were then extracted from S11 and S21 by extracting the resonance, frequency and efficiency components and following the previous characterization method.

2.7 Application for dielectric resonator

Important in areas such as food, horticulture and medical, military and defense. For example, in various zones. For these purposes, content representation techniques based on RF and microwave estimates have traditionally been used. These methodologies can be referred to as free-space projections, transmission lines and techniques based on resonance [1]. In view of the high precision, high sensitivity and low cost, resonance-based strategies are frequently favored [2]. This technique offers an inside information on material properties by changing the deliberate resonating recurrence and consistency factor by stacking a resonator.

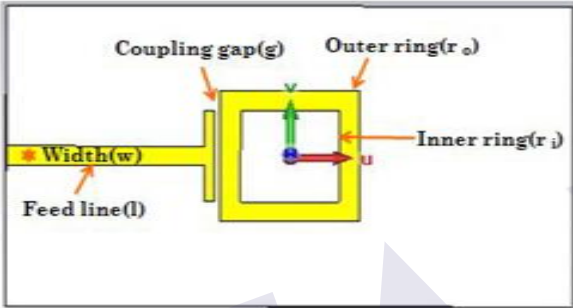
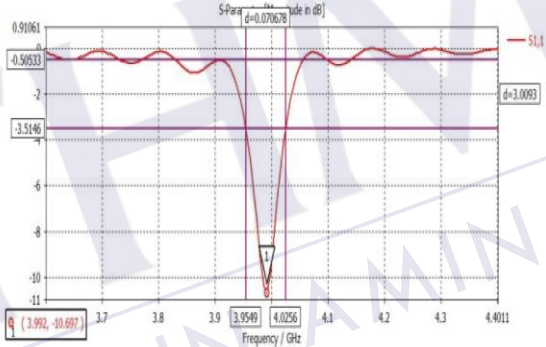
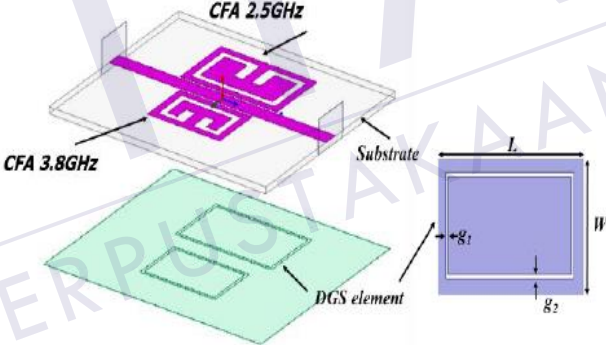
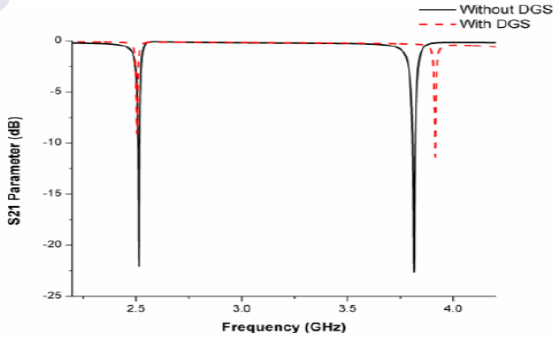
2.8 Previous Work Study

For previous project that related research that have been conducted by the researcher to design dielectric resonator, Table 2.1 will be Summarized of RELATED WORKS. Previous studies inform you the different studies

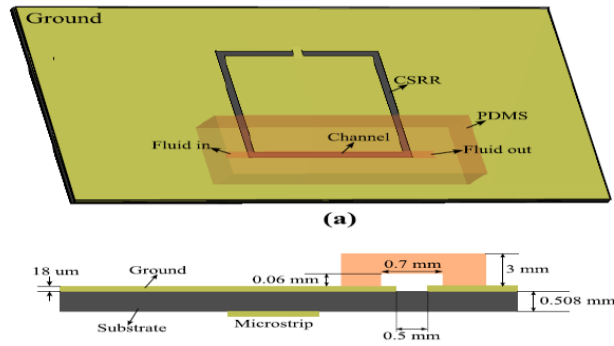
conducted in that field. They are important because they tell you how much research has been done, how it has been done & the outcomes. It also informs you that you cannot repeat the same thing as plagiarism would suggest. You should know what others have done before you study a subject.



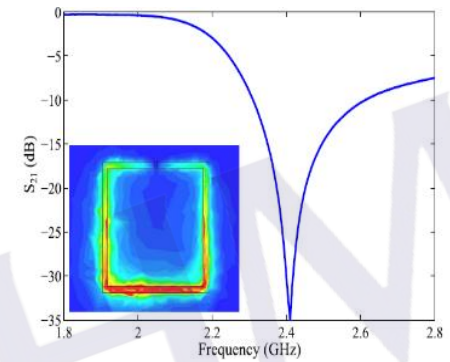
Table 2.1: Summary of literature review

| Author | Design | Material and Frequency | Result |
|---|---|--|--|
| <p>Rammah Alahnomi, Natasha Binti Abd Hamid, Zahriladha Zakaria, Tole Sutikno, Amyrul Azuan Mohd Baar</p> |  | <p>Substrate: Roger 5800 frequency: 4GHz</p> |  |
| <p>Norhanani Abd Rahman, Zahriladha Zakaria, Rosemizi Abd Rahim, Yosza Dasrill, Amyrul Azuan Mohd Bahar</p> |  | <p>Dual Band CFA with DGS structure Frequency: 2.5 and 3.8 GHz</p> |  |

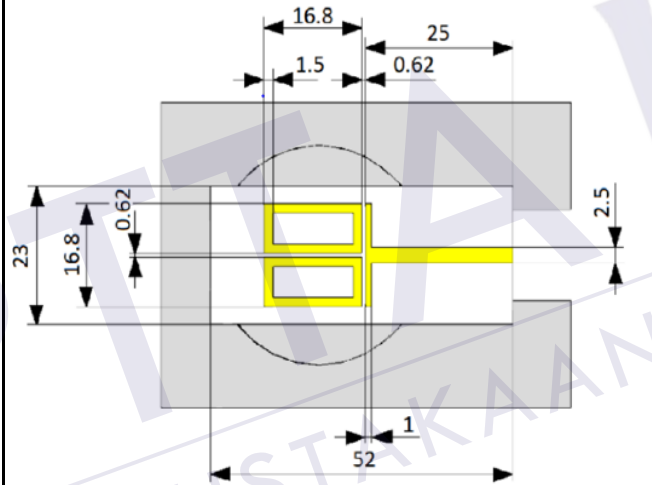
Amir Ebrahimi,
Withawat
Withayachumna
nkul,
Said Al-Sarawi,
and Derek
Abbott



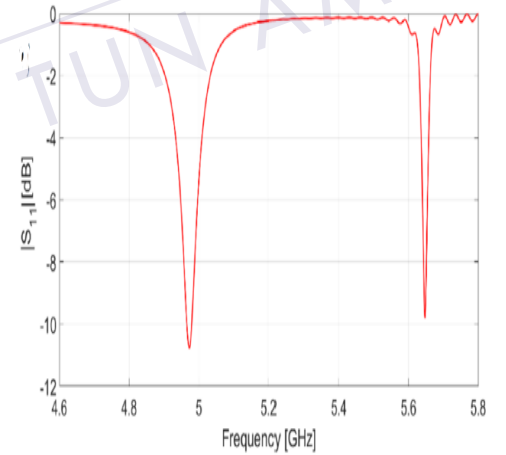
Rogers
RO6002
Frequency:
2.4 GHz



Aleksandr
Ivanov, Timur
Agliullin, Dario
Laneve,
Vincenza
Portosi,
Artem Vorobev,
Raoul R.
Nigmatullin,
Aydar
Nasybullin,
Oleg Morozov,
Francesco
Prudenzano,
Antonella
D’Orazio and
Marco Grande



Rogers
5880
Frequency:
5-5.6GHz



2.9 Summary

This chapter discussed the important part which is knowing what the title is about which is resonator and dielectric. First explanation on dielectric resonator types of dielectric resonator and method of dielectric resonator. Second the types of resonator and explaining it deeply. Third explaining the material and application used for it in real life. Lastly the previous work done. An artificially formed structure common to metamaterials is a split-ring resonator (SRR). Their goal is to achieve the desired magnetic susceptibility (magnetic response) of up to 200 terahertz in different metamaterial forms. There are a broader number of dividing rings and periodic designs: rod-split-rings, nested split rings, single split rings, deformed split rings, spiral split rings, and extended S-structures. Split-ring resonators have obtained different effects, including smaller and higher frequency structures. The metamaterial structure is studied in microwave frequencies in square split ring resonator (SSRR). The resonant frequency is determined by the mathematical study of the resonating structure.



PT TAAU THM
PERPUSTAKAAN TUNKU Tahir Aminah

CHAPTER 3

Research methodology

3.1 Introduction

In this part, split-ring resonator (SRR)- based sensor for dielectric characterization materials is proposed. The spotlight will predominantly be on the design and the specification and measurement utilizing CST software.

A split-ring resonator (SRR) based sensor for dielectric characterization materials is proposed. By and large, the activity of microwave resonance-based sensor pivots with respect to the shift in the resonance frequency and the adjustment in the quality factor of the loading structure.

By the examination of the measured resonance frequency and quality factor, simulated design to get the S_{11} and S_{21} and the sample of material under test (MUT) can be tested. In this project sample of material is mounted on the resonator most sensitive are to make sure the sensor work, only solid material is tested such as iron and wood

3.2 Flowchart

This project methodology is utilized to achieve the main goal of the project to perform the expected result. This method for this project will be based on S-SRR sensing design. Fig 3.1. Shown the flow chart of this project.

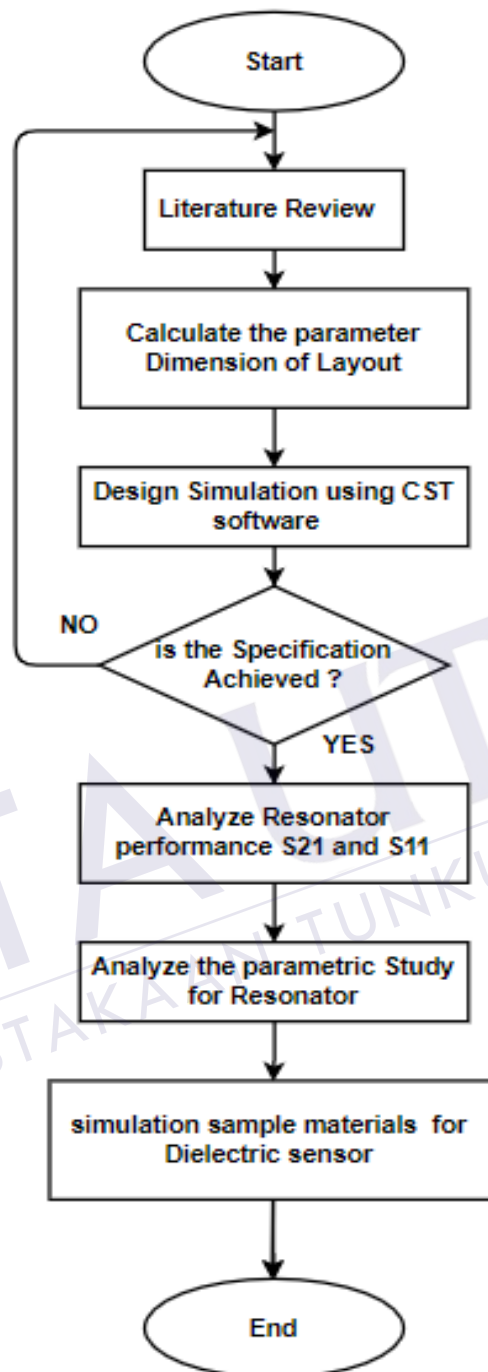


Figure 3:1 Flowchart of the project

3.3 Substrate Specification

The shaped of square SRR will be designed 2.45 GHz frequency and substrate specification in order to operate properly. This report presents the design of Square SRR for dielectric characterization. Table 3.1 shows the substrate and parameters specification design;

Table 3.1: Substrate Materials Specification

| Specification | Substrate FR4 |
|-----------------------------------|---------------|
| Characteristic impedance, Z_0 | 50Ω |
| Dielectric constant, ϵ_r | 3.38 |
| Thickness of substrate, h | 1.6 mm |
| Thickness of copper, t | 0.035mm |

3.4 Project Methodology

Towards completing this project, well planning is an essential element which makes all process of the project goes smoothly. Before starting with the designing process, few factors must be considered such as a technique for design square SRR for dielectric characterization, types of sensor response and feedline, formulas and the software that will be used. The suitable one will be selected as a method to design this project to meet the objectives of the project. All of these processes are illustrated clearly in flow chart in Figure 3.1.

3.4.1 Calculation

Circuit RLC whose frequency of resonance is provided with resonator

$$f_r = \frac{1}{2\pi\sqrt{LC}} \quad (1)$$

L and C are the corresponding resonator inductance and capability.

The relationship between the frequency shift and MUT content can be expressed as follows:

$$\frac{\Delta f_r}{f_r} = \frac{\int_V (\Delta \epsilon E_1 E_0 + \Delta \mu H_1 H_0) dv}{\int_V (\epsilon_0 / E_0^2 + \mu_0 / H_0^2) dv} \quad (2)$$

Where the air-filled (unloaded) resonant frequency is, the resonant frequency change, $\Delta \epsilon = \epsilon_0(\epsilon_r - 1)$ also $\Delta \mu = \mu_0(\mu_r - 1)$ are Changes in the permittivity and permeability of free space, and the electrical and magnetic field without MUT loading are the interrupted fields and V is the interrupted length.

By specifying the element of quality $Q = f_r / \Delta f_{3dB}$,

where f_r is the resonance frequency and Δf_{3dB} is the unloaded sensor displays an efficiency factor of 145, - 3dB bandwidth.

The actual part of the permeability is written according to the normalized resonance frequency with the curve fitting technique:

$$\mu_r = \frac{2.443 f_{rn}^2 - 5.696 f_{rn} + 3.464}{f_{rn}^2 - 0.7414 f_{rn} - 0.04783} \quad (3)$$

where f_{rn} is the normalized resonance frequency. The following numerical model was established with the curve fitting tool:

$$\tan \delta_m = 6.731 - 55.81 \mu_r + 31.05 Q_n^{-1} + 16.57 \mu_r^2 + 4.902 \mu_r Q_n^{-1} - 0.3784 Q_n^{-2} \times 10^{-3} \quad (4)$$

where Q_n is the normalized quality factor.

$$\epsilon_r = \frac{-399.3 f_{rn}^2 - 765.8 f_{rn} + 1234}{f_{rn}^2 + 243.4 f_{rn} - 176.3} \quad (5)$$

Where the resonance frequency of f_{rn} is normalised.

The method was used to precisely write the electrical loss tangent of MUT according to the reverse normalised quality factor and the magnetic loss tangent, which resulted in actual permittivity:

$$\tan \delta_e = (p_1 + p_2 Q_n + p_3 \varepsilon_r + p_4 Q_n^2 + p_5 Q_n \varepsilon_r + p_6 \varepsilon_r^2 + p_7 Q_n^3 \varepsilon_r + p_8 Q_n^2 \varepsilon_r + p_9 Q_n \varepsilon_r^2) \times 10^{-3} \quad (6)$$

Where Q_n is the uniform quality factor and p_1, p_2, p_3, p_4, p_5 and p_6 are true permittivity functions.

SSRR specification equations:

$$f_0 = \frac{1}{2\pi\sqrt{LC}} \quad (7)$$

$$L = \mu_0 a_m \left(\ln \frac{8a_m}{h+c} - 0.5 \right) \quad (8)$$

$$a_m = a + w/2 \quad (9)$$

$$C_g = \varepsilon \left(\frac{ch}{g} + \frac{2\pi h}{\ln \left(\frac{2.4h}{c} \right)} \right) \quad (10)$$

$$C_{surf} = \frac{2\varepsilon_0 h}{\pi} \ln \left(\frac{4a}{g} \right) \quad (11)$$

$$\frac{1}{C} = \frac{1}{C_g} + \frac{1}{C_{surf}} \quad (12)$$

f_0 = resonant frequency

L = The inductance can be approximated by that of a closed ring

μ_0 = is the permeability of free space

a_m = is the mean radius of the ring

C_{surf} = surface capacitance

C_g = The gap in the ring corresponds to capacitance

3.4.2 Simulation

There are few important things need to be determined before start designing in CST 2019 Microwave Studio and those important things are the dimension and layout of the filter, the material to be used and the characteristic of the material. For the substrate, FR4 is used with thickness $h = 1.6$ mm and relative dielectric constant, $\epsilon_r = 3.38$. The dimension of the sensor and the layout of resonator is calculated to suite the desired frequency range.

First step in designing filter in CST is to draw the substrate material, ground and Square SRR with feedlines for the dielectric. For this project, FR4 will be used as substrate and copper for ground and the ring with feedlines. The substrate, ground can be designed using brick function.

Table 3.2: The specification of the SRR

| Specification | Value |
|---------------------|-------------|
| Substrate | FR4 |
| Thickness | 1.6 mm |
| Copper thickness | 0.035 |
| Operating frequency | 2.45 GHz |
| Impedance | 50 Ω |

3.4.3 Square split Ring Resonator

Figure 3.2 shows the layout for substrate and ground. The size of ground and substrate is 45.53 mm x 70 mm. The material use for substrate is FR4 and the thickness is 1.6 mm assigned in brick function. For ground plane, use copper as material and the thickness is 0.035 mm assigned in brick function. Table 3.4 show the specification of ring and feedline.

Table 3.4 Specification of ring and feedline

| No | Name | Dimension (mm) |
|----|---------------------|----------------|
| 1 | Ring Length, L | 34 |
| 2 | Ring Width, W | 34 |
| 3 | Feedline Length, L1 | 6 |
| 4 | Feedline Width, W1 | 17.93 |
| 5 | Feedline gap | 0.07 |

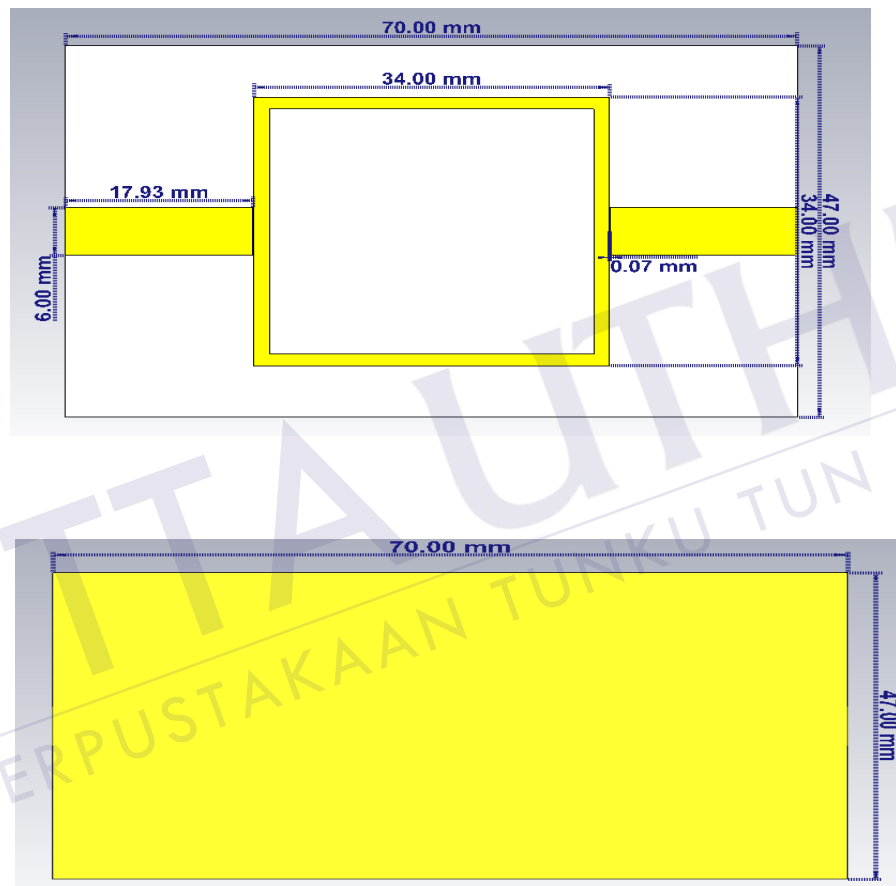


Figure 3.2: (a) Substrate (b) ground of basic SSRR

Figure 3.2 show the specifications of the substrate, the ring and feedline. Copper is used as material shows the value for width and length 34mm x 34 mm for the ring and feedline 17.9mm x 6mm with input impedance 50Ω , frequency 2.45.

3.4.4 Square Split Ring Resonator with Gap

Figure 3.3 shows the layout for substrate and ground. The size of ground and substrate is 45.53 mm x 70 mm. The material use for substrate is FR4 and the thickness is 1.6 mm assigned in brick function. For ground plane, use copper as material and the thickness is 0.035 mm assigned in brick function. Table 3.5 show the specifications of ring, ring gap and feedlines, feed gap.

Table 3.5 Specification of square ring with gap

| No | Name | Dimension (mm) |
|----|------------------------|----------------|
| 1 | Ring Length, L | 34 |
| 2 | Ring Width, W | 34 |
| | Ring gap | 0.18 |
| 3 | Feedline Length, L_1 | 6 |
| 4 | Feedline Width, W_1 | 17.93 |
| 5 | Feedline gap | 0.07 |

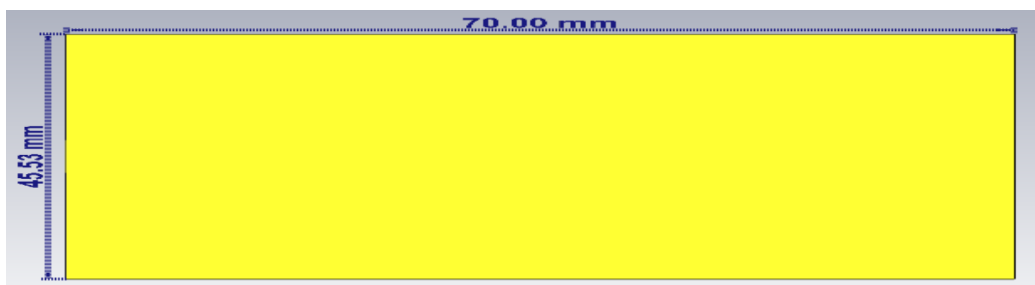
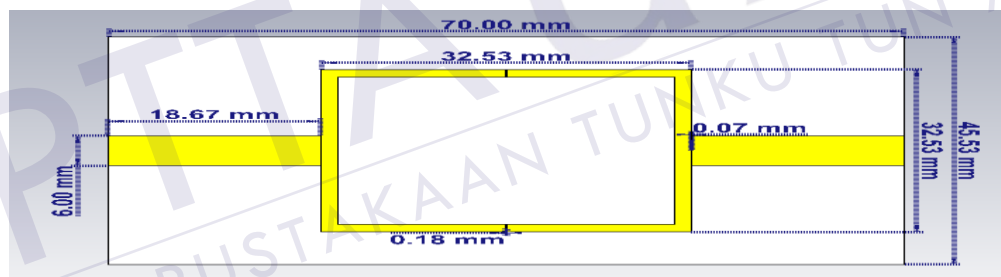


Figure 3.3: (a) Substrate (b) Ground split ring resonator.

The second step is to design the Square SRR and feedlines. Figure 3.3 shows that copper is used as material shows the value for width and length

39.53mm x 39.53mm for the ring and feedline 18.67mm x 6mm feedline gap 0.07mm and ring gap 0.18mm with input impedance 50Ω , frequency 2.45.

3.4.5 Split Ring Resonator Technique

We present a systematic numerical study, approved by went with test information, of single square split ring resonators of a single ring with no hole, two holes. We examine the conduct of the magnetic resonance frequency.

In this work, Square split-ring resonator transmission properties are investigated at frequencies without any split and double-split transmissions. In the different E and H field polarisations, the dissipating parameters of devices are studied. The magnetic resonance of E and H fields is known and the variations in the conduct of resonators are clarified based on simulation and experimental findings due to the directions of the fields.

Different designs of the exciting vectors are considered to expand the two divisions of the system. There is an indistinguishable transmission quality in no divisions, as verified with simulations and investigation, and in the two-split resonators for an unique excitement design. The introduced resonators can function properly for changing exciting conditions as a frequency selective media.

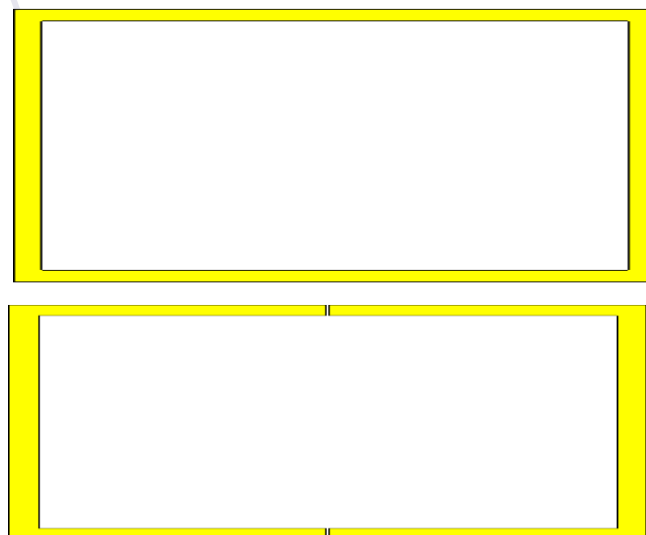


Figure 3.4: (a) Basic SRR (b) modified SRR.

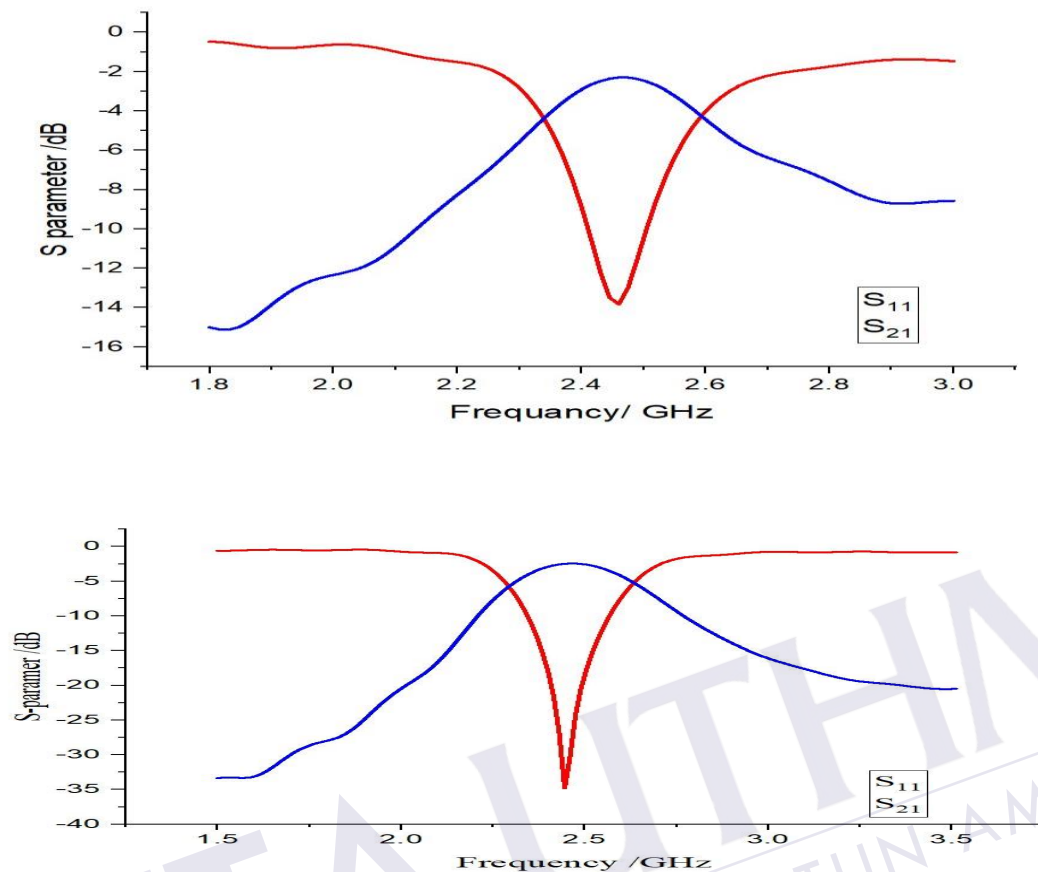


Figure 3.5: S parameter (a) Basic (b) modified SRR.

3.5 Dielectric Characterization Design for Material

The sensor design is about material testing on dielectric characterization based on this two materials wood and iron and comparing them with the original before MUT. The testing mechanism that used in this study is simulating SRR before and after MUT. Sample is placed on where the density of H field is the highest. It makes the obtained result to be more accurate. After finishing all the simulations the result of the S_{11} will be compared with all different material.

Figure 3.6 shows the design without Material Under Test (MUT).

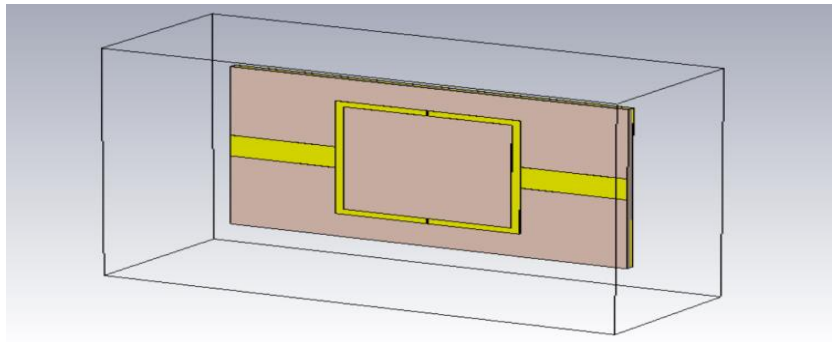


Figure 3.6: Original design.

Figure 3.7 shows the design after Material under Test (MUT), which is cube of iron placed on upper side square split ring resonator S-SRR at its most sensitive area of the sensor.

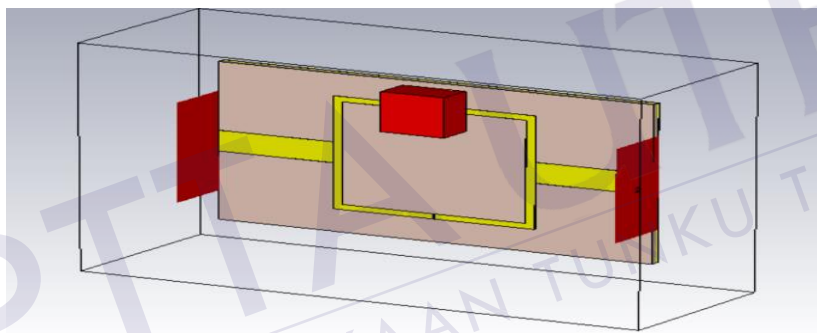


Figure 3.7: Iron sample for MUT

Figure 3.8 shows the design after Material under Test (MUT), which is cube of wood placed on upper side square split ring resonator S-SRR at its most sensitive area of the sensor.

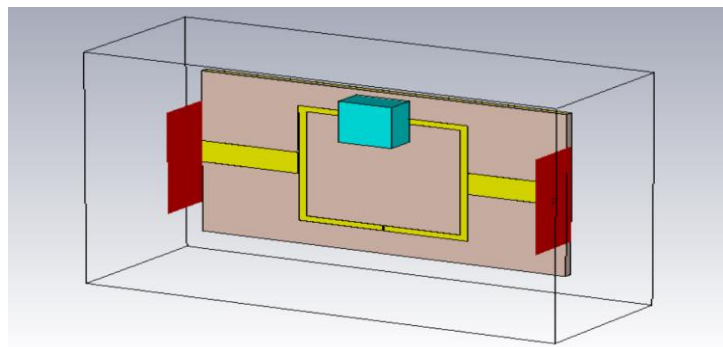


Figure 3.8: Wood sample for MUT

CHAPTER 4

Result and discussion

4.1 Introduction

The result achieved from the software plus prototype for Square SRR for dielectric characterization. For this project, the results are divided into two types of results, which are simulation results. The results will be compared to the simulated material sample. The simulation results is being discussed in term of frequency and gain, by using CST 2019 Microwave Studio software.

4.2 Simulation Result and Discussion

Simulation is an important method before the production process that can help to evaluate the best dielectric characterization and sensor property measurement configuration for the SRR in simulation initially based on frequency levels and design S parameter. Based on the analysis as shown in Figure 4.1 where the begin proposed design layout in 2.45GHZ using SRR.

4.2.1 Square split Ring Resonator

Figure 4.1 shows the basic Square SRR layout of sensor designed using CST 2019 Microwave Studio. The design starts with the single square SRR with feedline on both sides. The yellow region where consist of feedline and Square SRR is copper and the white region is substrate.

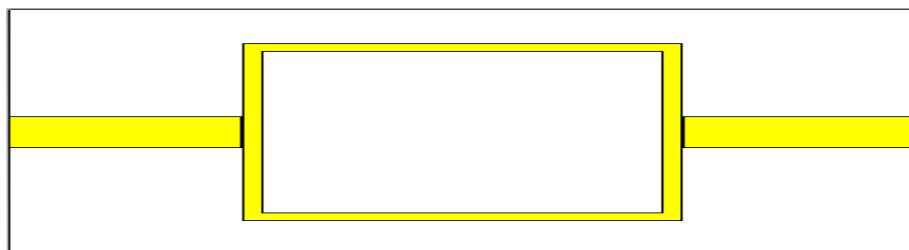


Figure 4.1: Square SRR

The value of dimension is from CST. Start with width and length of square ring 34mm x34mm, the feedline width $W= 17.93\text{mm}$ and length $L= 6\text{mm}$ the gap between feedlines and the Square ring feed gap = 0.07mm, impedance of $50\ \Omega$.

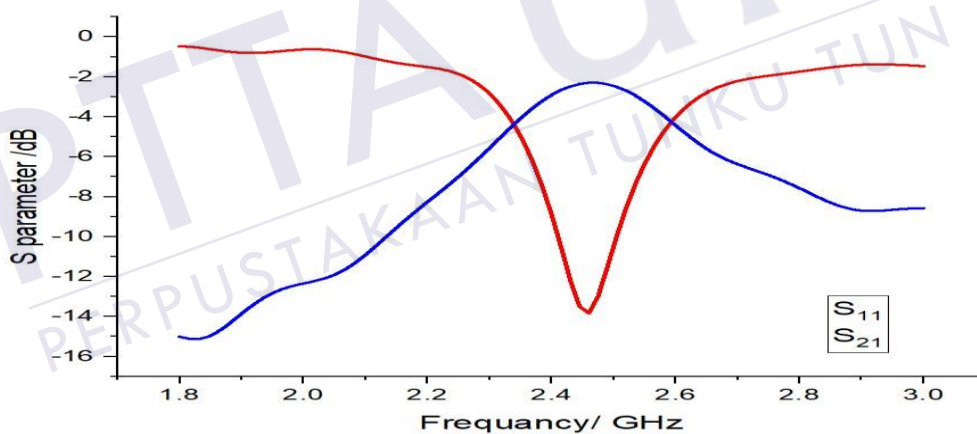


Figure 4.2: Simulated S-parameter Square SRR

4.1.2 Square Split Ring Resonator with gap

Figure 4.3 shows the modified Square SRR design. The modified process same parameter dimension of basic Square SRR. Start with adding

gap in ring on both sides, the parameter dimensions the length and width of the ring 32.53mm x 32.53mm, the ring gap = 0.009mm.

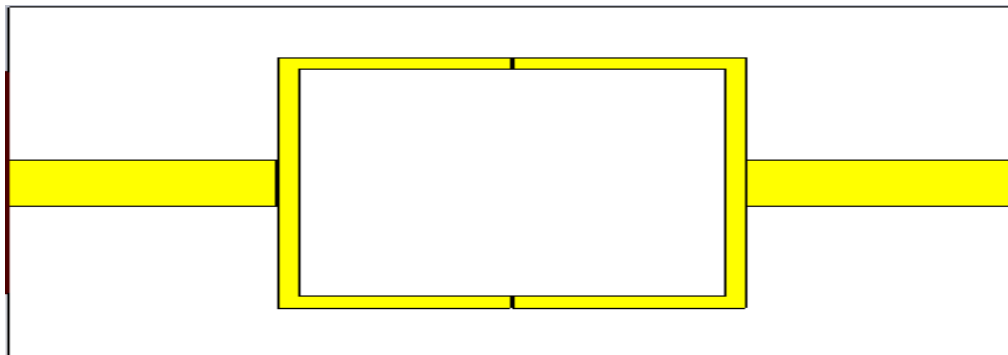


Figure 4.3: Modified Square SRR

Figure 4.4 shows the simulated s-parameter response of modified single Square SRR. From the graph it can see that the result is close to basic design of Square SRR with better S_{11} and S_{21} because the parameter dimension is same, just difference shaped with additional gap on both sides of the ring. Therefore, after modified the shaped of Square SRR, the simulated result of modified Square SRR frequency is 2.45 GHz with S_{11} -35 dB and S_{21} -2.5dB.

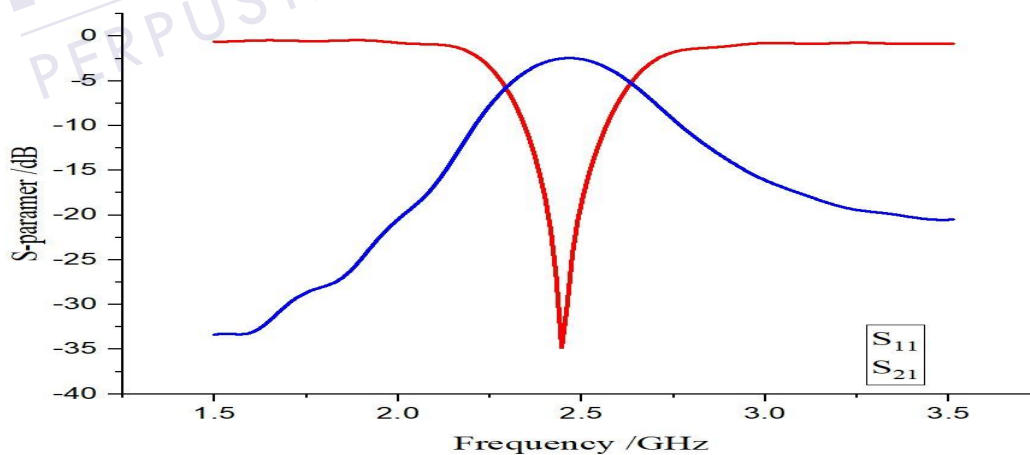


Figure 4.4: Simulated S-parameter of Modified Square SRR.

4.3 Current Distribution

It is interesting to note that the current distribution for the square ring. From Figure 4.5, it is concluded that the use of a via to ground on ring resonators gives the additional advantage of size reduction compared to the conventional ring resonators.

The resonator's square geometry and relatively short side length support the current trajectory of Figure 4.5. In contrast to previous cases the lengths of the real loops are shorter. Therefore, the magnetic resonance frequency. As a consequence of the electric field together with the Resonator the second resonant frequency of 2.45 GHz is due.

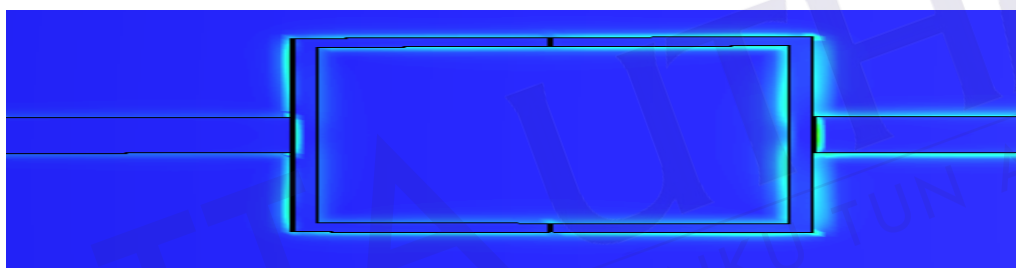


Figure 4.5: Distribution of electric field at the Square SRR frequency of 2.45 GHz.

4.4 H-field and E-field distribution of the Square split Ring Resonator

The volume permeability will dramatically alter the frequency of the resonance. Thus the permeability is to be determined independently of its permittivity by stacking this resonator volume with a MUT sample.

Again, the permittivity of the sample may be established from the change in the resonant frequency, unless the permeability of the sample is calculated, by piling a sample MUT in a resonator volume where the electric field is confined with a high strength. To accomplish such “single-field localized” areas. A SRR sensor is intended when the SRR is electrically linked to a 50-microstrip line via connections to the ground plane. A FR4 cover was applied as a substratum with a 3.38 dielectric constant and a 1,6

mm thickness. Figure 4.6 displays the SRR stacked feedline S_{21} . The picture exhibits a resonance of 2.45 GHz.

The resonance frequency H and E circulations are shown in Fig. 4.8 Split, shows a high H strength and almost zero E in the area used as a detection area for permeability. Then again, E is located with maximum intensity in a district shown as the primitive detector field, although H is irrelevant. These two regions are most appropriate spot for the samples of the dielectric characterization.

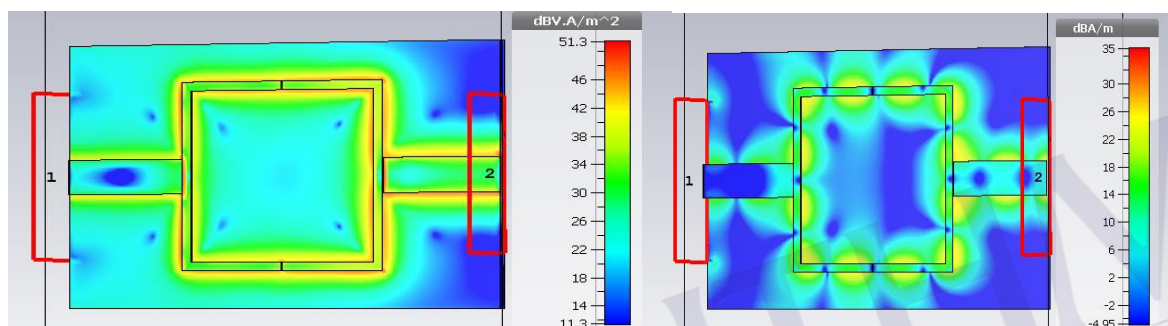


Figure 4.6 Permeability and Permittivity sensing area

4.5 Square split Ring Resonator Parametric study analysis

Table 4.1 shows the variation length of modified single Square SRR. The length and width of the ring 32.53mm x 32.53mm, the ring gap = 0.18mm. Based on the parametric study of Square SRR gap to monitor the change of S_{11} and S_{21} .

Table 4.1: Parametric study of Ring gap

| No | Ring gap (mm) | Frequency (GHz) | S_{11} (dB) | S_{21} (dB) |
|----|---------------|-----------------|---------------|---------------|
| 1 | 0.08 | 2.45 | -24 | -2.06 |
| 2 | 0.09 | 2.45 | -35 | -2.5 |
| 3 | 0.1 | 2.45 | -22.8 | -2.46 |
| 4 | 0.11 | 2.45 | -18.2 | -2.85 |
| 5 | 0.12 | 2.45 | -15.6 | -3.2 |

Figure 4.7 shows the simulated result of S-parameter after parametric study of ring gap, which stays at the same frequency but changes S11 and S21. The best gain will be at ring gap = 0.09mm.

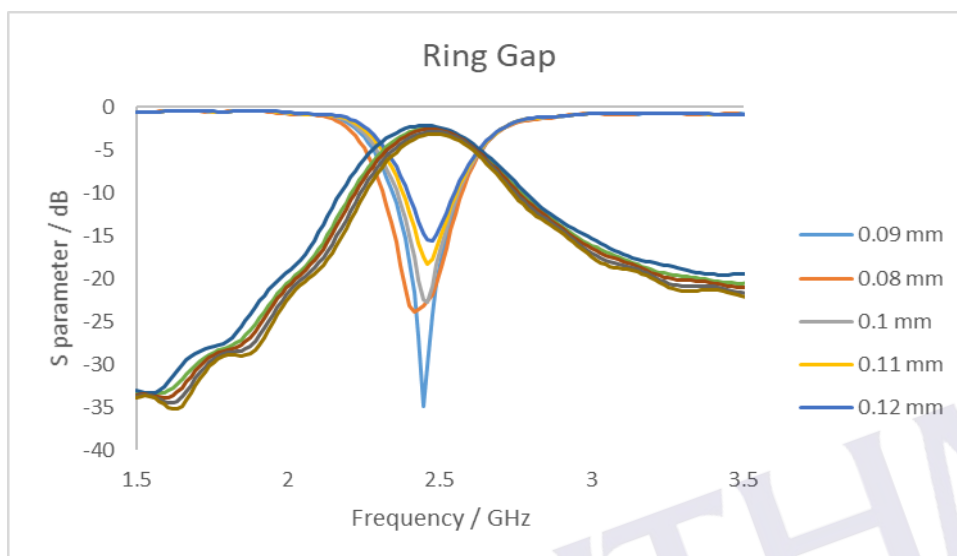


Figure 4.7: Simulated S-parameter parametric study of ring gap.

Table 4.8 shows the parametric study of feedline gap. By changing the gap between the feedline and the ring to get different S parameter but same frequency. The best result will be at feedline gap = 0.07mm.

Table 4.2: Parametric study of feedline gap

| No | Feed gap | Frequency (GHz) | S ₁₁ (dB) | S ₂₁ (dB) |
|----|----------|-----------------|----------------------|----------------------|
| 1 | 0.07 | 2.45 | -35 | -2.5 |
| 2 | 0.08 | 2.45 | -18.97 | -2.34 |
| 3 | 0.09 | 2.45 | -15.22 | -2.72 |
| 4 | 0.1 | 2.45 | -13.3 | -3.02 |
| 5 | 0.11 | 2.45 | -12.1 | -3.6 |

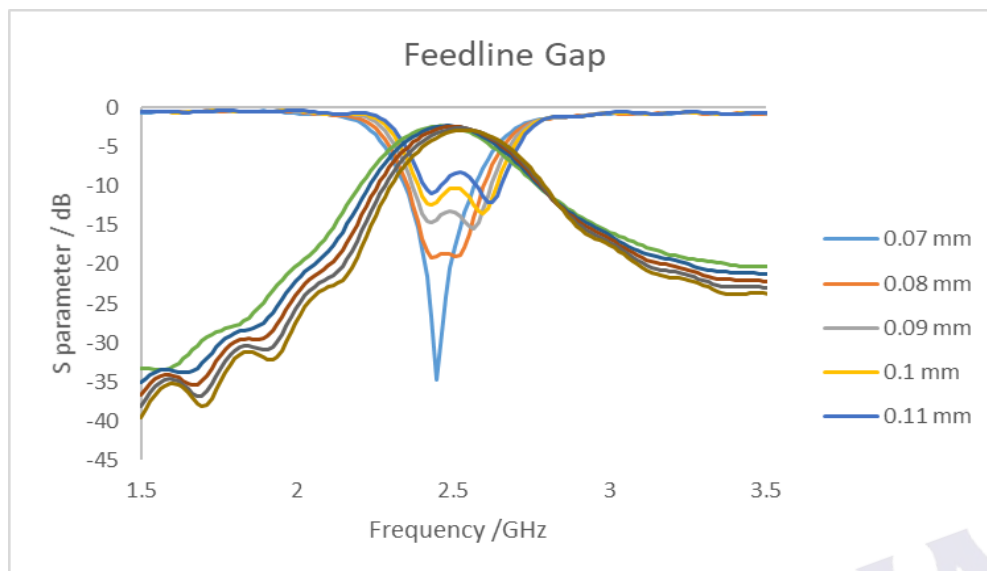


Figure 4.8: Simulated S-parameter parametric Study of feedline gap.

Table 4.9 shows the parametric study of Ring width. By changing the ring width to get different S11 and S21 but same frequency. The best result will be at ring width = 1.5 mm.

Table 4.3: Parametric study of Ring width

| No | Ring width (mm) | Frequency (GHz) | S11(dB) | S21(dB) |
|----|-----------------|-----------------|---------|---------|
| 1 | 1.5 | 2.45 | -35 | -2.5 |
| 2 | 2 | 2.45 | -19.5 | -2.22 |
| 3 | 1 | 2.45 | -16.4 | -2.8 |
| 4 | 0.5 | 2.45 | -10.4 | -3.8 |

Figure 4.9 shows the simulated S-parameter for parametric study of Ring width and the change that happens in S11 and S21.

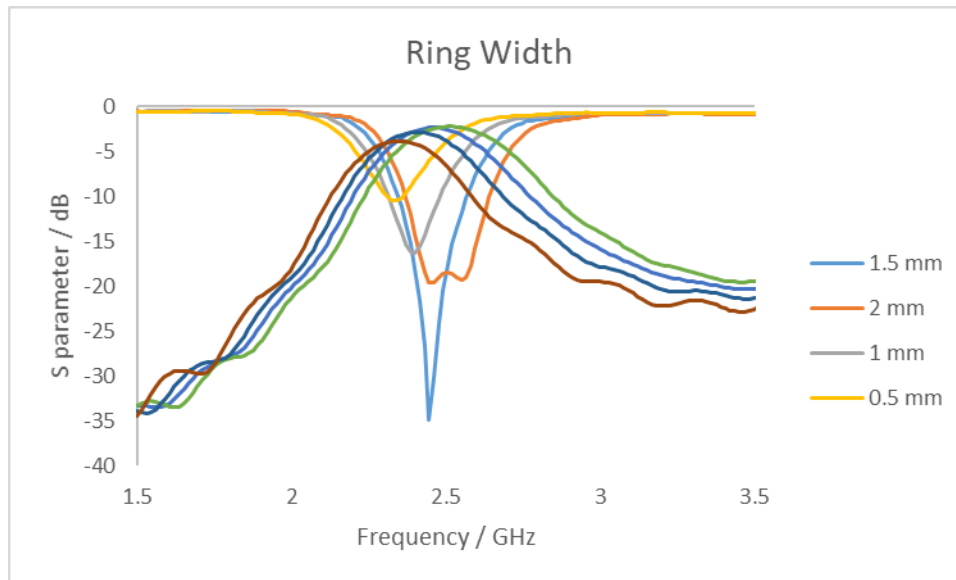


Figure 4.9: Simulated S-parameter parametric Study of Ring width

4.6 Result of dielectric characterization for materials

In order to verify the final design there are testing mechanism that has applied by using different material with different permittivity. The verification method conducted by using CST software where sample is mounded on final SRR design. The sample is positioned on the most sensitive area of the SRR. Result of the simulation shows the original frequency shifts depending on the type of the testing material that has been mounted on the SRR. All that shows the SRR is functioning as sensor to the permittivity and permeability of the material.

The Figure 4.10 show the result of dielectric characterization before MUT with frequency of 2.45 GHz with S11 at -35dB.

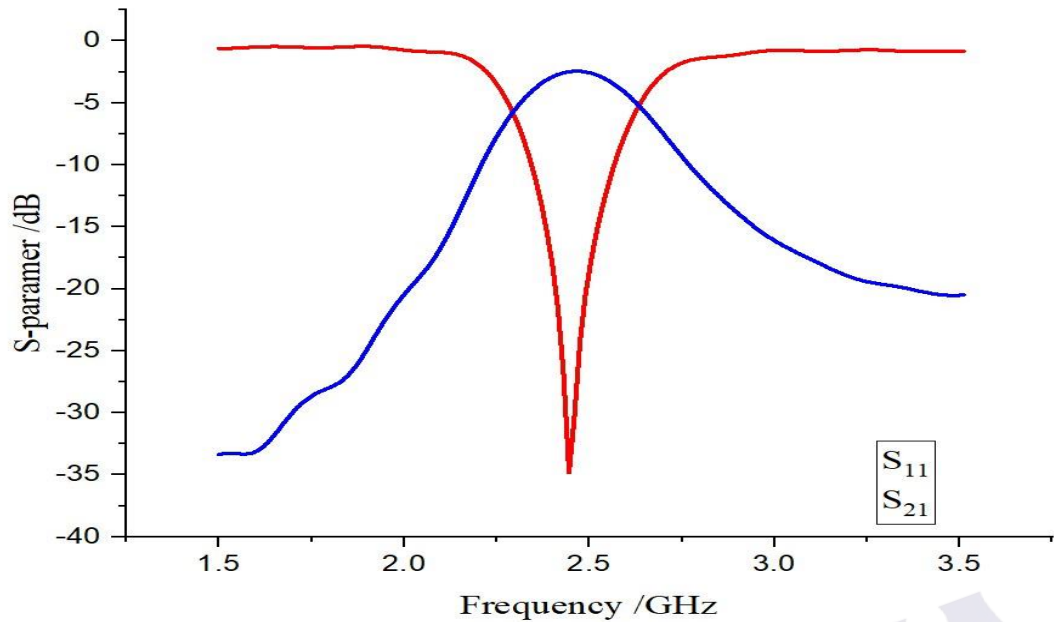


Figure 4.10: The result before MUT

The Figure 4.11 shows the result of S_{11} and S_{21} when SRR is mounted with Iron sample. That makes the frequency to shift from 2.45 GHz with -35dB to 2.26 GHz with -13dB. This verifies the the SRR design is working as sensor.

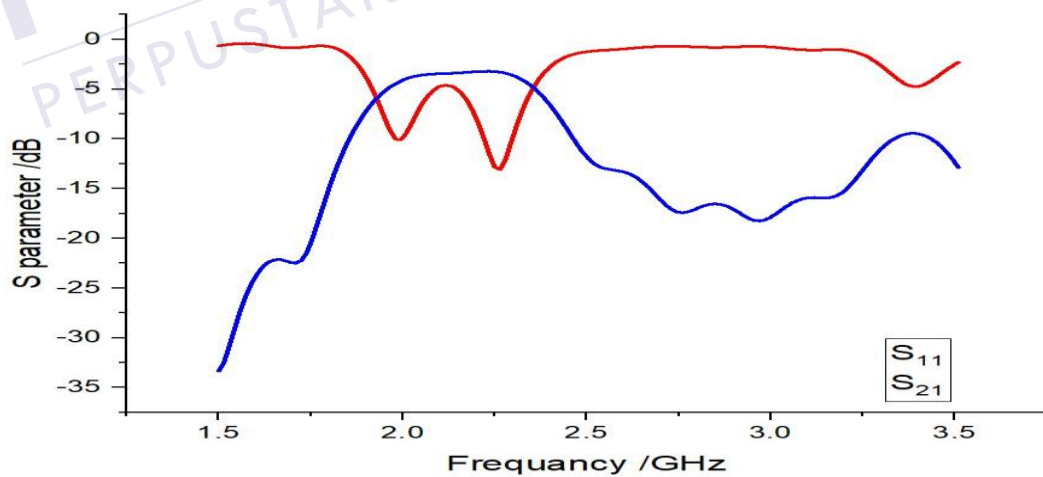


Figure 4.11: The simulation after the iron sample tested

The Figure 4.12 shows the result of S_{11} and S_{21} when SRR is mounted with wood sample. That makes the frequency to shift From 2.45 GHz with -35dB to 2.497 GHz with -23.6dB. This verifies the the SRR design is working as sensor.

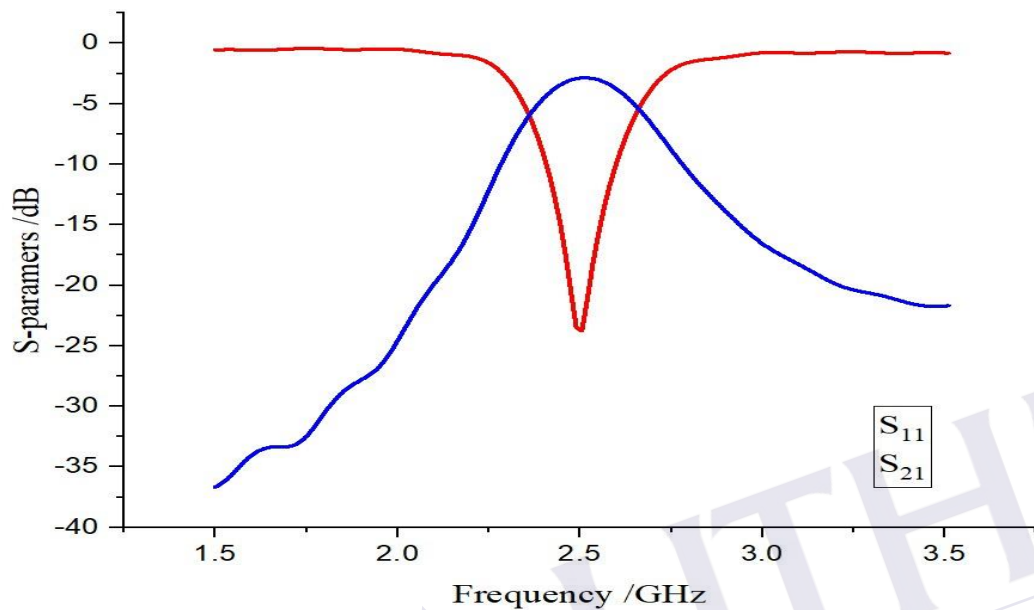


Figure 4.12: The simulation after wood sample tested

The Figure 4.13 and Figure 4.14 shows the comparison of materials iron and wood samples after the MUT with the original result before MUT. The clear shift of S_{11} shows the effectiveness of SRR as sensor.

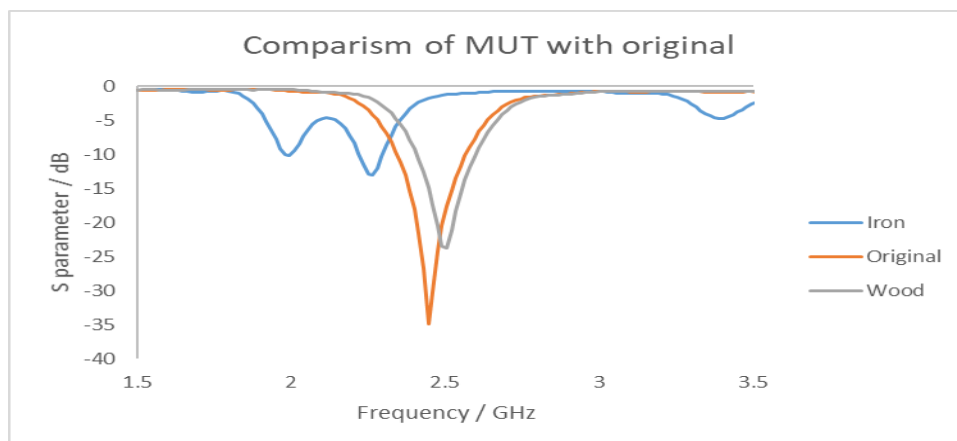


Figure 4.13: S_{11} Comparing the result of material before and after MUT.

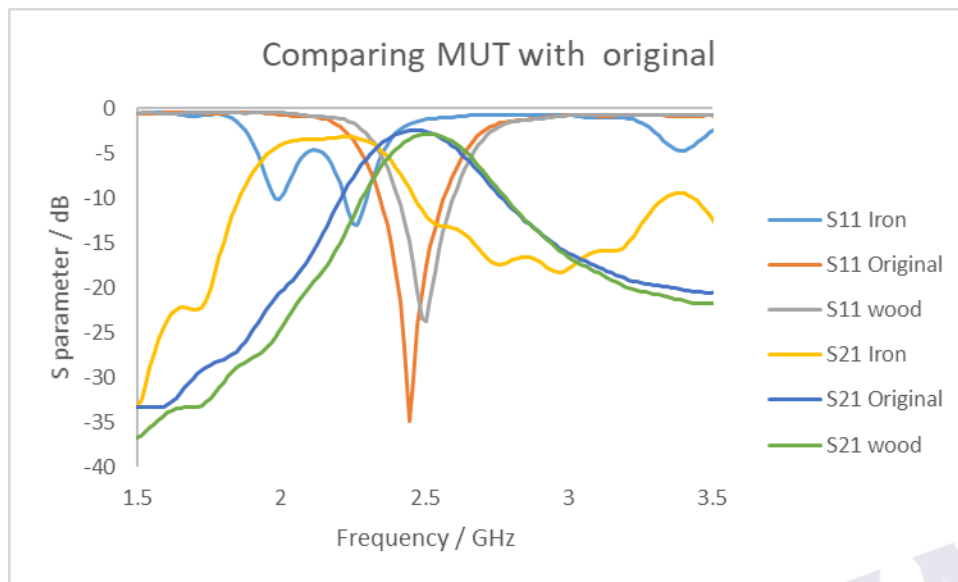


Figure 4.14: Compare of before and after MUT.

Two samples that are selected for study are iron and wood each being the testing sample. The S11 curves of the two samples has shifted along with that of the test SRR as reference. It is observed that the resonant frequencies are shifted towards lower and higher frequencies in relation to their permittivity values. This shift is in agreement with the results predicted by various numerical and simulation methods.

The resonant frequency of the SRR is observed to be 2.45 GHz. Out of the two samples used, the minimum frequency shift is for iron and maximum is for wood. The corresponding resonant frequencies observed are 2.497 GHz and 2.26 GHz, respectively.

CHAPTER 5

Conclusion

5.1 Summary

In this project, the characterization material sensor based on S-SRR was introduced. The proposed sensor has advantages and cost-effective and simplicity in the preparation of samples. S-SRR limiting electrical and magnetic fields was designed in two different zones by testing the field appropriation on the resonator.

The region of high intensity containing the electric field yet delicately using the magnet field to detect the MUT electrical permittivity. By inserting MUT samples in these detection areas and evaluating the resonance frequency change and the consistency factor of the sensor unloaded. Sensor was developed and applied to differentiate individual dielectric and magnetic materials. A good understanding was observed between the developed findings and the reference data. In CST simulation, Iron and wood are used for MUT changes the frequency the Iron which makes the frequency shift from 2.45 GHz with -35dB to 2.26 GHz with -13dB, Wood which makes the frequency shift From 2.45 GHz with -35dB to 2.497 GHz with -23.6dB.

The s-parameter response of modified single Square SRR. From the graph it can see that the result is close to basic design of Square SRR with better frequency because the parameter dimension is same, just difference shaped with additional gap on both sides of the ring. So, after modified the shaped of Square SRR better frequency. The simulated result of modified Square SRR frequency is 2.45 GHz with of S_{11} -35 dB and S_{21} -2.5dB.

5.2 Recommendation

For future recommendation of Single Square split ring resonator is try with more rings to see how good of results. Second, is using another substrate that suits with high frequency if we can get a smaller size of resonator where can reduce the production cost and integrate which other device and a good performance by comparing with this project output. Next, design the SRR, SRR has different shapes such as u shape circle shape etc., which each have their unique sensitivity and give good frequencies. Lastly, for the dielectric characteristic MUT in this project applied solid material such as Iron and Wood for future work other materials can be tested liquid, gas.



PTTA UTHM
PERPUSTAKAAN TUNKU TUN AMINAH

REFERENCES

- [1] R. Mirzavand, M. M. Honari, and P. Mousavi, "High-resolution balanced microwave material sensor with extended dielectric range," *IEEE Trans. Ind. Electron.*, vol. 64, no. 2, pp. 1552–1560, Feb. 2017.
- [2] S. Trabelsi and S. O. Nelson, "Microwave sensing of quality attributes Of agricultural and food products," *IEEE Instrum. Meas. Mag.*, vol. 19, no. 1, pp. 36–41, Feb. 2016.
- [3] B. Milovanovic, S. Ivkovic, and V. Tasic, "A simple method for permittivity measurement using microwave resonant cavity," in *Proc. 12th Int. Conf. Microw. Radar. (MIKON) Conf.*, vol. 3, May 1998, pp. 705–709.
- [4] K. Saeed, R. D. Pollard, and I. C. Hunter, "Substrate integrated waveguide cavity resonators for complex permittivity characterization of materials," *IEEE Trans. Microw. Theory Techn.*, vol. 56, no. 10,
- [5] T. Shimizu, S. Kojima, and Y. Kogami, "Accurate evaluation technique of complex permittivity for low-permittivity dielectric films using a cavity resonator method in 60-GHz band," *IEEE Trans. Microw. Theory Techn.*, vol. 63, no. 1, pp. 279–286, Jan. 2015.
- [6] R. A. Alahnomi, Z. Zakaria, E. Ruslan, A. A. M. Bahar, and S. R. A. Rashid, "High sensitive microwave sensor based on symmetrical split ring resonator for material characterization," *Microw. Opt. Technol. Lett.*, vol. 58, pp. 2106–2110, Sep. 2016.
- [7] R. A. Alahnomi, Z. Zakaria, E. Ruslan, S. R. Ab Rashid, and A. A. M. Bahar, "High-Q sensor based on symmetrical split ring resonator with spurlines for solids material detection," *IEEE Sensors J.*, vol. 17, no. 9, pp. 2766–2775, May 2017.
- [8] J. Dong, et al., "Noncontact measurement of complex permittivity

- of electrically small samples at microwave frequencies,” *IEEE Trans. Microw. Theory Techn.*, vol. 64, no. 9, pp. 2883–2893, Sep. 2016.
- [9] A. A. M. Bahar, Z. Zakaria, S. R. Ab Rashid, A. A. M. Isa, and R. A. Alahnomi, “High-efficiency microwave planar resonator sensor based on bridge split ring topology,” *IEEE Microw. Wireless Compon. Lett.*, vol. 27, no. 6, pp. 545–547, Jun. 2017.
- [10] R. Mirzavand, M. M. Honari, and P. Mousavi, “High-resolution balanced microwave material sensor with extended dielectric range,” *IEEE Trans. Ind. Electron.*, vol. 64, no. 2, pp. 1552–1560, Feb. 2017.
- [11] S. Trabelsi and S. O. Nelson, “Microwave sensing of quality attributes of agricultural and food products,” *IEEE Instrum. Meas. Mag.*, vol. 19, no. 1, pp. 36–41, Feb. 2016.
- [12] Keysight Technologies. Basics of Measuring the Dielectric Properties of Materials. Accessed: Jan. 2018. [Online]. Available: <http://literature.cdn.keysight.com/litweb/pdf/5989-2589EN.pdf>
- [13] S. P. Chakyar, S. K. Simon, C. Bindu, J. Andrews, and V. P. Joseph, “Complex permittivity measurement using metamaterial split ring resonators,” *J. Appl. Phys.*, vol. 121, no. 5, p. 054101, Feb. 2017.
- [14] Altschuler, H. (1963). Dielectric constant, In: *Handbook of Microwave Measurements*, Vol. 2, M. Sucher & J. Fox, (Eds.), pp. 530-536, Polytechnic Press, New York (NY), ISBN B-0011007T-C.
- [15] Athey, T., Stuchly, M., & Stuchly, S. (1982). Measurement of radio frequency permittivity of biological tissues with an open-ended coaxial line: Part I. *IEEE Transactions on Microwave Theory and Techniques*, Vol. 30, No. 1, (January 1982), pp. 82-86, ISSN 0018-9480.
- [16] Baker-Jarvis, J., Vanzura, E., & Kissick, W. (1990). Improved technique for determining complex permittivity with the transmission/reflection method. *IEEE Transactions on Microwave Theory and Techniques*, Vol. 38, No. 8, (August 1990) pp. 1096-1103, ISSN 0018-9480.
- [17] Benoit, E., Prot, O., Maincent, P., & Bessiere, J. (1996). Applicability of dielectric measurements in the field of pharmaceutical formulation. *Bioelectrochemistry and Bioenergetics*, Vol. 40, No. 2, (August 1996), pp. 175-179, ISBN 0302-4598.

- [18] Bernard, P., & Gautray, J. (1991). Measurement of dielectric constant using a microstrip ring resonator. *IEEE Transactions on Microwave Theory and Techniques*, Vol. 39, No. 3, (March 1991), pp. 592-595, ISSN 0018-9480.
- [19] Bogosanovich, M. (2000). Microstrip patch sensor for measurement of the permittivity of homogeneous dielectric materials. *IEEE Transactions on Instrumentation and Measurement*, Vol. 49, No. 5, (October 2000), pp. 1144-1148, ISSN 0018-9456.
- [20] Bryant, G. (1993). *Principles of microwave measurements*, Peregrinus on behalf of Institution of Electrical Engineers, ISBN 0-83641296-3, London (UK).
- [21] Cassivi, Y., Perregrini, L., Arcioni, P., Bressan, M., Wu, K., & Conciauro, G. (2002). Dispersion characteristics of substrate integrated rectangular waveguide. *IEEE Microwave and Wireless Components Letters*, Vol. 12, No. 9, (September 2002), pp. 333-335, ISSN 1531-1309.
- [22] Chen, L., Ong, C., Neo, C., Varadan V. V., & Varadan, V. K. (2004). *Microwave electronics: Measurement and materials characterization*, John Wiley and Sons, ISBN 0-47084492-2, Chichester (UK).
- [23] Deslandes, D., & Wu, K. (2001). Integrated microstrip and rectangular waveguide in planar form. *IEEE Microwave and Wireless Components Letter*, Vol. 11, No. 2, (February 2001), pp. 68-70, ISSN 1531-1309.
- [24] Deslandes, D., & Wu, K. (2001). Integrated transition of coplanar to rectangular waveguides, *Proceedings of IEEE MTT-S International Microwave Symposium (Vol. 2)*, ISBN 0-78036538-0, Phoenix (AZ), May 2001.
- [25] Edwards, T., & Steer, M. (1991). *Foundations of interconnect and microstrip circuit design (3rd ed.)*, John Wiley and Sons, ISBN 0-47160701-0, New York (NY)
- [26] Facer, G., Notterman, D., & Sohn, L. (2001). Dielectric spectroscopy for bioanalysis: From 40 Hz to 26.5 GHz in a microfabricated waveguide. *Applied Physics Letters*, Vol. 78, No. 7, (February 2001), pp. 996-998, ISSN 1077-3118.
- [27] Fratticcioli, E., Dionigi, M., & Sorrentino, R. (2004). A simple low cost measurement system for the complex permittivity characterisation of

materials. IEEE Transactions on Instrumentation and Measurement, Vol. 53, No. 4, (August 2004), pp. 1071-1077, ISSN 0018-9456.

